The Journal of Experimental Biology 215, 2760-2773

doi:10.1242/jeb.068122

RESEARCH ARTICLE

Spectral tuning by selective chromophore uptake in rods and cones of eight populations of nine-spined stickleback (*Pungitius pungitius*)

Pia Saarinen*,†, Johan Pahlberg*,‡, Gábor Herczeg, Martta Viljanen, Marika Karjalainen, Takahito Shikano, Juha Merilä and Kristian Donner

Department of Biosciences, University of Helsinki, P.O. Box 65, FI-00014 Helsinki, Finland

*These authors contributed equally to this work
†Author for correspondence (pia.k.saarinen@helsinki.fi)
‡Present address: Department of Physiology and Biophysics, Zilkha Neurogenetic Institute, University of Southern California, Los Angeles, CA 90089, USA

SUMMARY

The visual pigments of rods and cones were studied in eight Fennoscandian populations of nine-spined stickleback (*Pungitius pungitius*). The wavelength of maximum absorbance of the rod pigment (λ_{max}) varied between populations from 504 to 530 nm. Gene sequencing showed that the rod opsins of all populations were identical in amino acid composition, implying that the differences were due to varying proportions of chromophores A1 and A2. Four spectral classes of cones were found (two S-cones, M-cones and L-cones), correlating with the four classes of vertebrate cone pigments. For quantitative estimation of chromophore proportions, we considered mainly rods and M-cones. In four populations, spectra of both photoreceptor types indicated A2 dominance (population mean λ_{max}=525–530 nm for rods and 535–544 nm for M-cones). In the four remaining populations, however, rod spectra (mean λ_{max}=504–511 nm) indicated strong A1 dominance, whereas M-cone spectra (mean λ_{max}=519-534 nm) suggested substantial fractions of A2. Quantitative analysis of spectra by three methods confirmed that rods and cones in these populations use significantly different chromophore proportions. The outcome is a shift of M-cone spectra towards longer wavelengths and a better match to the photic environment (light spectra peaking >560 nm in all the habitats) than would result from the chromophore proportions of the rods. Chromophore content was also observed to vary partly independently in M- and L-cones with potential consequences for colour discrimination. This is the first demonstration that selective processing of chromophore in rods and cones, and in different cone types, may be ecologically relevant.

Supplementary material available online at http://jeb.biologists.org/cgi/content/full/215/??/????/DC1

Key words: rhodopsin, porphyropsin, photoreceptor, visual ecology.

Received 11 November 2011; Accepted 10 April 2012

INTRODUCTION

The absorptance spectrum of a visual pigment describes how efficiently it catches photons of different energies (light of different wavelengths) to initiate vision. For pigments serving vision near absolute threshold (rod pigments in most vertebrates), optimal properties can be defined rather simply: the pigment should maximize the signal-to-noise ratio (SNR) by absorbing efficiently the light wavelengths (photon energies) available in the environment, but at the same time be thermally stable to minimize spontaneous activations, i.e. noise (Barlow 1956; Baylor et al., 1980). Because spectral and thermal properties are interdependent (Barlow 1957; Ala-Laurila et al., 2004a; Ala-Laurila et al., 2004b; Luo et al., 2011), optimal positioning of the absorbance spectrum will often imply a trade-off between these two demands. The spectral positioning of cone visual pigments, however, is often best considered in relation to wavelength discrimination rather than absolute sensitivity (Barlow 1958; Vorobyev and Osorio, 1998; Vorobyev et al., 2001a; Vorobyev et al., 2001b). Cones generally operate in brighter light where photon fluctuations constitute the most powerful source of pigment-initiated noise, hence thermal stability of the visual pigment may be less crucial.

All visual pigments are G-protein coupled receptors with a light-catching cofactor (the chromophore) covalently bound to the protein (opsin). Spectral absorbance and thermal stability depend on the interaction of the opsin and the chromophore, and may be tuned by modifying either component (Bridges, 1972; Hargrave et al., 1983; Nathans, 1990a; Nathans, 1990b; Yokoyama and Yokoyama, 2000). Evolutionary adaptation to different light regimes by opsin-based tuning (fixation of new mutations by natural selection) is a fairly slow process, typically requiring at least 10^3–10^4 generations (Terai et al., 2006; Jokela-Määttä et al., 2005; Jokela-Määttä et al., 2009; Larmuseau et al., 2009; Larmuseau et al., 2010). Admittedly, in some fishes, differential expression of multiple genes in the same photoreceptors, e.g. during different stages of life history, provides a mechanism for 'fast' opsin-dependent tuning of spectral sensitivity (Shand 1993; Browman and Hawryshyn 1994; Archer et al., 1995; Hope et al., 1998; Carleton and Kocher 2001; Shand et al., 2002; Spady et al., 2005; Spady et al., 2006; Parry et al., 2005).

Chromophore-based tuning in vertebrates implies changing proportions of two alternative chromophores, A1 (11-*cis* retinal) and A2 (11-*cis* 3,4-didehydroretinal), an option available to fish, amphibians and some reptiles (see Bridges, 1972). The capacity for

chromophore-based tuning is genetically determined (requiring conversion of A1 into A2 by a retinol dehydrogenase), but when present, it allows tuning pigments on a physiological time scale, e.g. seasonally (Beatty, 1975; Temple et al., 2006) or for different stages of life history (Wald, 1946; Carlisle and Denton, 1959; Reuter, 1969; Reuter et al., 1971). The A1 to A2 switch red-shifts and broadens the absorption spectrum (Dartnall and Lythgoe, 1965; Whitmore and Bowmaker, 1989; Hárosi, 1994; Govardovskii et al., 2000; Parry and Bowmaker, 2000; see also Bridges, 1972) by lowering the energy barrier for activation, and is always associated with a decrease in thermal stability of the pigment (Ala-Laurila et al., 2004a; Ala-Laurila et al., 2004b; Ala-Laurila et al., 2007; Luo et al., 2008; Luo et al., 2011).

The Baltic and Fennoscandian region provides a 'natural laboratory' for the study of visual evolution in aquatic animals, offering multiple populations of several species that have become isolated in water bodies with different spectral properties following the retreat of Pleistocene ice sheets during the past ~9000 years (Donner, 1995; Eronen et al., 2001). Here, we have studied to what extent and by what mechanisms the visual pigments of nine-spined sticklebacks (*Pungitius pungitius*) have diverged spectrally in five freshwater and three marine populations. The questions we addressed were: (1) are there differences in the rod opsin that might underlie differential tuning of the rod visual pigment; (2) do sticklebacks use chromophore-based tuning of the visual pigments and, if so, are there consistent differences between populations in this respect; and (3) if rod and/or cone visual pigments differ between populations, can the differences be functionally interpreted as enhancing some aspects of visual performance in the illumination conditions now prevailing in their respective habitats?

MATERIALS AND METHODS

Animals

Nine-spined sticklebacks [*Pungitius pungitius* (Linnaeus 1758)] from eight Fennoscandian populations were used, four of which were Finnish (Rytilampi, Pyöreälampi, Iso-Porontima and Helsinki), two Swedish (Abborrtjärn and Bölesviken) and two Russian (Levin Navolok and Mashinnoye; see Fig. 1). Henceforth, we shall denote the populations by three-letter abbreviations as shown on the map. Three of the habitats (HEL, BOL and WHI) were brackish or saltwater environments, whereas five were freshwater ponds (RYT, PYO, ABB and MAS) or lakes (ISO). Most of these populations have been reproductively isolated for the past 8000 years or so (Eronen et al., 2001), except for MAS, which has been separated from WHI for less than a century. On the basis of microsatellite data, the MAS population is indistinguishable from WHI, whereas those of all other ponds and lakes are very different from any other population (Shikano et al., 2010). The sea and freshwater populations, including MAS, already show distinct morphological, behavioural, neuroanatomical and life history adaptations, presumably chiefly in response to reduced predatory pressure in isolated ponds lacking predatory fish (Gonda et al., 2011; Herczeg et al., 2009a; Herczeg et al., 2009b; Herczeg and Välimäki, 2011; Trokovic et al., 2011).

After capture in June, the fish were transferred in tanks to the animal care facilities at the University of Helsinki, kept in aerated freshwater aquaria at approximately 15°C under a 12 h:12 h light:dark cycle (in a windowless room with fluorescent tubes) and provided with appropriate food. All fish studied by microspectrophotometry (MSP) were kept in these constant conditions for more than 6 months before recordings were carried out in the following year (see below). The experiments were authorized by the Animal Experiment Board at the University of Helsinki and the National Animal Experiment Board of Finland.

Fig. 1. Geographic locations of the habitats of the eight populations studied: Abborrtjärn (ABB), Bölesviken (BOL), Helsinki (HEL), Iso-Porontima (ISO), Mashinnoye (MAS), Pyöreälampi (PYO), Rytilampi (RYT) and White Sea at Levin Navolok (WHI). Sea habitats are marked by blue stars, ponds by yellow stars and the lake by a red star.

DNA analyses

The gene coding for the protein (opsin) part of the rod visual pigment was sequenced to see whether there was any variation in coding sequences. Total genomic DNA of three individuals from each of the eight populations was extracted using NaOH boiling (Duan and Fuerst, 2001). Teleost primers were kindly provided by Prof. David Hunt (Lions Eye Institute, University of Western Australia) and Dr Wayne Davies (Nuffield Laboratory of Ophthalmology, Oxford University), designed for nested PCR to amplify the fragments containing the transmembrane part of the rod opsin gene: 5′-ACAGAGGGACCCTHYTTYTAYRTCCCYATG-3′ RH1_F1, 5′-CATCCTBVTBGGHTTYCCCRTCAACTTCCT-3′ RH1_F2, 5′-CTTCCCRCAGCACADKGTGGTGAKCATGCA-3′ RH1_R1 and 5′-GCTGGARGASRCDGADGARGCCTCGGTCTT-3′ RH1_R2. The primer order is 5′…F1…F2…R1…R2…3′ so the possible primer combinations and amplicon sizes are as follows: F1–R2, 1038 bp; F1–R1, 966 bp; F2–R1, 835 bp; and F2–R2, 907 bp.

Initial PCR consisted of 1× Phire Reaction Buffer [20 mmol l^{-1} Tris-HCl, 0.1 mmol l^{-1} EDTA, 1 mmol l^{-1} DTT, 100 mmol l^{-1} KCl, stabilizers, 200 μg ml^{-1} bovine serum albumin (BSA) and 50% glycerol; ThermoFisher Scientific, Waltham, MA, USA], 0.2 mmol l^{-1} of each dNTP (ThermoFisher Scientific), 5 pmol of primers F1 and R2, 0.2 μl of Phire Hot Start I DNA Polymerase (ThermoFisher Scientific) and approximately 10 ng of DNA in the final reaction volume of 10 μl. The temperature profile consisted of preliminary denaturation at 98°C for 30 s followed by 30 cycles of 98°C for 10 s, 48°C for 10 s, 72°C for 30 s and final extension at 72°C for 1 min. Nested PCR was conducted with 1:20 diluted F1+R2 amplicon as a template with the same protocols (exception: 25 cycles instead of 30) for primer pairs F1–R1, F2–R1 and F2–R2. PCR products were then incubated for 30 min at 37°C with 5 U of Antarctic Phosphatase (New England Biolabs, Ipswich, MA, USA), 50 U of Exonuclease I (New

England Biolabs), 1× Antarctic Phosphatase Buffer and 1× Exonuclease I Buffer. Cycle sequencing reactions were run with the BigDye Terminator v1.1 Cycle Sequencing Kit (Applied Biosystems, Carlsbad, CA, USA) according to the manufacturer's instructions. Fragments were cleaned with the Montage SEQ96 Sequencing Reaction Cleanup Kit (Merck Millipore, Billerica, MA, USA) before running them in capillary electrophoresis (MegaBACE, GE Healthcare, Piscataway, NJ, USA). Sequences were aligned using MEGA 5 (Tamura et al., 2011) and deposited in GenBank (accession numbers JQ619637–JQ619638).

Microspectrophotometry

Absorbance spectra of visual pigments were recorded by MSP in single outer segments of rods and cones. All fish used for MSP were adult individuals of average length (4–6 cm). Koli (Koli, 1990) reports that the typical length of sexually mature Finnish nine-spined sticklebacks is 3–5 cm, but fish from ponds are generally somewhat bigger than fish from the sea. Recordings were obtained in 2008 in all eight populations: in February–April for ABB, ISO, PYO, RYT, BOL and HEL, and in August–October for WHI and MAS (data from 47 individuals). In 2011, additional samples from the populations HEL, PYO and RYT were studied in January–June (data from 22 individuals); further, two more RYT individuals were studied in autumn 2011. The numbers of individuals (*N*) studied in each population in the two years, and the months of recording, are given in Table 1. The replications in 2011 served two purposes. Firstly, it was essential to check how constant the properties were of each population, especially the differences in chromophore ratios between populations, over two different years for fish that had been treated similarly and studied at roughly the same time of the year. Secondly, preparation procedures during 2008 were carried out under dim red light (λ>650 nm). Although this light will have negligible effect on rods and on short- and middle-wavelength-sensitive cones (S- and M-cones, respectively), it will bleach the visual pigment of long-wavelength-sensitive cones (L-cones) to varying extent. In 2011, all procedures were carried out under infrared light (LED with peak emission at 850 nm and 50 nm half-bandwidth) with the aid of an infrared viewer.

Table 1. Wavelengths of peak absorbance and chromophore content in rods and M-cones in eight populations of nine-spined stickleback

Data set	Population and recording season (*N*)	Photoreceptor type (*n*)	Template λ_{max} (±s.e.m.)	A1 (%)	PCA component peak	Percent explained
1	Abbortjärn / ABB (6) 2/2008	Rod (107)	507.8±0.6	97.6	501.8	38.3
		Cone (126)	519.2±0.7	70.6	516.8	58.1
2	Iso-porontima / ISO (5) 2/2008	Rod (137)	511.0±1.4	84.6	503.5	57
					571.4	2.7
		Cone (75)	523.3±1.7	60.5	515.8	59.1
					580.6	2.4
3	Pyöreälampi / PYO (6) 4/2008	Rod (108)	504.8±0.4	92.5	504.5	60.0
		Cone (59)	518.6±0.6	68.4	526.2	60.0
					515.2	7.6
4	Pyöreälampi / PYO (7/6) 2–5/2011	Rod (225)	507.9 ±0.6	96.2	507.2	65.9
					574.2	1.0
		Cone (131)	534.3±1.8	39.7	532.5	77.0
					519.8	7.1
					546.8	4.9
					589.5	2.6
5	Rytilampi / RYT (6) 2–3/2008	Rod (180)	507.9±1.5	90.1	500.8	60.0
					560.8	2.3
		Cone (108)	520.3±1.0	73.1	517.4	66.9
6	Bölesviken / BOL (7/6) 2/2008	Rod (153)	527.6±1.3	19.6	523,0	41.3
		Cone (92)	541.7±1.6	4.1	535.5	45.6
7	Helsinki / HEL (5) 3/2008	Rod (98)	527.3±1.4	5.4	–	–
		Cone (78)	538.0±2.7	35.5	–	–
8	Helsinki / HEL (8/6) 1–5/2011	Rod (251)	529.0±0.6	11.2	525.2	79.0
		Cone (242)	544.8±2.3	23.1	530.5	66.9
					618.5	1.1
9	White Sea / WHI (5/3) 4–10/2008	Rod (112)	528.6±1.4	50.8	536.2	54.2
					569.9	5.6
		Cone (31)	536.0±1.1	12.4	523.8	35.1
					536.3	16.3
10	Mashinnoye / MAS (6) 8–9/2008	Rod (145)	529.5±0.6	7.3	525.4	45.6
		Cone (95)	543.5±1.0	3.1	535.1	34.3
11	Rytilampi / RYT (6) 3–5/2011	Rod (148)	516.5±3.2	62.7	513.5	66.8
					569.2	2.1
		Cone (212)	540.6±1.6	36.2	534.2	61.6
					603.5	2.1

The populations are divided into two groups according to chromophore dominance in rods: group 1 (data sets 1–5), with A1-dominated rods; and group 2 (data sets 6–0), with A2-dominated rods.

See Results for comments on data set 9 (WHI), and data set 11 (RYT).

N, number of individuals included; *n*, total number of cells from which spectra are included; λ_{max}, Govardovskii et al. (Govardovskii et al., 2000) parameter obtained by fitting sums of A1 and A2 templates to the full spectrum of each individual; A1 (%), percentage of A1 calculated as the mean of estimates obtained by the two independent methods 1 and 2 (see Materials and methods).

Results of principal component analysis (PCA) are shown as the peak wavelengths of major PCA components, and percent of the total variance explained by each of them (method 3).

Before experiments, the fish to be used was kept in complete darkness for at least 2 h (usually longer, for up to 24 h). The fish was then decapitated and the brain and spinal cord were destroyed with a preparation needle. The pelvic fins were cut off and stored in absolute ethanol for later genomic analyses. The eyes were enucleated and one eye was stored in formalin for morphological analyses. The other eye was hemisected in teleost Ringer's solution (110 mmol l^{-1} NaCl, 2.5 mmol l^{-1} KCl, 1 mmol l^{-1} $CaCl_2$, 1 mmol l^{-1} $MgSO_4$, 10 mmol l^{-1} $NaHCO_3$, 10 mmol l^{-1} glucose and 10 mmol l^{-1} HEPES, pH≈7.5). The central part of the isolated retina (detached from the pigment epithelium) was transferred to a drop of Ringer's solution on a microscope slide and teased apart to isolate photoreceptors and expose their outer segments. Dextran (relative molecular mass=66,900) was added to the Ringer's solution to immobilize cells during measurements. The sample was covered with a coverslip, sealed at the edges with Vaseline to prevent drying, and put on the MSP stage.

Absorbance spectra were recorded with a single-beam, computer-controlled, fast wavelength-scanning microspectrophotometer built at the University of Helsinki according to the basic design of Govardovskii and Zueva (Govardovskii and Zueva, 1988; Govardovskii and Zueva, 2000). The recordings were made at room temperature from single outer segments of rods and cones, which could be distinguished morphologically. Each cell was measured only once. The size of the measuring beam was adjusted to fit the outer segment, typically the whole length and ¾ of the width, although the full width was used in small cone outer segments to maximize SNR. The beam was linearly polarized in the plane of the discs. The wavelength calibration was checked at the beginning and end of each experiment against the spectrum of a 'blue glass' standard (Schott BG20, Mainz, Germany), which had been accurately measured in a Hitachi spectrophotometer. The data were stored on a computer hard disk and the basic processing was as described by Govardovskii et al. (Govardovskii et al., 2000). Raw spectra from single cells were averaged and normalized for each individual separately, and in case there was obvious zero offset and/or drift, the spectra were corrected by fitting a new baseline through points at long wavelengths, where absorbance was negligible, >650 or >700 nm depending on cell type. (This was not possible in A2-dominated L-cones.) Further technical details can be found in Govardovskii et al. and Ala-Laurila et al. (Govardovskii et al., 2000; Ala-Laurila et al., 2002).

Our main analysis is focussed on rods and M-cones (see below). Recordings from both classes of photoreceptors were obtained from 69 individuals. Rods were very abundant and on average 20–30 good rod spectra were collected from each individual. The total number of spectra from single rods included in the analyses is 1761. The M-cone spectra obtained from the same individuals were also averaged from recordings of 20–30 cells each, with a total of 1489 single-cell spectra included in the analyses. S-cones were much less abundant and had smaller outer segments. Therefore, S-cone spectra were obtained from only 55 of the 69 individuals, typically averaged from five to 10 cells in each (359 S-cones in total). Sampling of L-cone spectra in 2008 was unrepresentative, as especially the A2 version of the visual pigment was bleached by the red preparation light (see above). In 2011, when only infrared light was used, spectra were obtained from 210 L-cones with population mean λ_{max} ranging from 551 to 602 nm, and only these were used for quantitative analysis.

Analysis of spectra

Even if only a single opsin is present, analysis of spectra of an A1:A2 mixture entails determination of two unknown variables, λ_{max} of either component and the A1:A2 proportion. In the following, we generally express the former variable in terms of λ_{max}(A1), whereby λ_{max}(A2) is fixed by Hárosi's (Hárosi, 1994) formula for the general relation first described by Dartnall and Lythgoe (Dartnall and Lythgoe, 1965), hereafter termed the DLH relationship, and the latter as A1 percentage, A1(%). For a theoretical, noise-free spectrum, it would be possible to find a unique solution by fitting sums of standard A1 and A2 pigment templates, relying on the fact that the component spectra differ in shape (see Govardovskii et al., 2000). For noisy spectra, however, fits of approximately equal quality may be achieved with different value pairs [λ_{max}(A1), A1(%)]. Within certain limits, increasing one and decreasing the other have rather similar effects on the shape of the mixed spectrum. When applied to recorded spectra, where different portions may be affected by quite different types of noise, the ambiguity cannot be resolved by any statistical procedures. Disambiguation by prior assumptions, in contrast, will introduce systematic error. Our strategy was therefore to use two essentially independent methods that rely on different subsets of the spectral data, and are not sensitive to the same sources of systematic error. Our final conclusions rely on the consistency of results obtained by these two methods. As a third method providing additional insight, we applied principal component analysis (PCA).

Method 1: template fitting and determination of chromophore content based on the shape of spectra

Sums of A1 and A2 templates of Govardovskii et al. (Govardovskii et al., 2000) in varying proportions were fitted to the α-band of normalized, averaged and zero-line corrected spectra of each individual (see above). Fitting implies setting the two parameters λ_{max}(A1) and A1(%) by iterative toggling until finding a best fit, as judged by eye on the computer screen. It is important to note that method 1 relies almost entirely on the sloping parts of spectra and is insensitive to data points around the peak (see Fig. 2). Moreover, it makes no prior assumptions on λ_{max}(A1) or λ_{max}(A2). These two properties make it independent of method 2, described next.

Method 2: determination of chromophore content from the wavelength of peak absorbance

The wavelength of peak absorbance of a mixture of A1 and A2 pigments based on the same opsin is fully defined by the proportions of the two components and their λ_{max}. If either λ_{max}(A1) or λ_{max}(A2) is known (mutually coupled by the DLH relationship), A1(%) can be calculated from the λ_{max} of the mixture. To make method 2 formally independent of method 1, we did not use the λ_{max} value obtained by template fitting, but used an estimate based exclusively on data around the peak. These estimates (here denoted λ_{maxp}) were obtained by least-square fitting of second-order polynomials (parabolas) to data points ±30 nm and ±50 nm around the template-based λ_{max}, which was used only as a provisional anchoring point (cf. Ala-Laurila et al., 2002). The two vertex values (λ_{v30} and λ_{v50}) thus obtained were averaged to give $\lambda_{maxp}=(\lambda_{v30}+\lambda_{v50})/2$. Estimating A1(%) requires that λ_{max}(A1) or λ_{max}(A2) be fixed by some independent assumption. As there is no way of knowing how close any single measurement may be to a 'pure' component, fixing these end points is the main source of potential systematic error of method 2. For rods, the lower and upper bounds of population mean λ_{max} were 504.8 and 529.5 nm, respectively. If these represented pure A1 and pure A2, respectively, the complementary values according to the DLH relationship would be λ_{max}(A2)=531.5 nm and λ_{max}(A1)=503.3 nm. Thus the observed range is sufficiently close to the DLH prediction to warrant the conclusion that the observed

population boundaries in rods correspond to nearly pure A1 and A2. For M-cones, however, the population extremes were 519.0 and 543.5 nm, defining a range much narrower than predicted from their respective DLH complements λ_{max}(A2)=555 nm and λ_{max}(A1)=512.5 nm. Thus, only one of the observed boundaries (at best) can correspond to pure A1 or pure A2. Because the highest value, 543.5 nm, was found in two highly A2-dominated populations (MAS and HEL), and other A2-dominated populations were close to that (see Results), we fixed M-cone λ_{max}(A2) at 543.5 nm, giving λ_{max}(A1)=512.5 nm.

Fig. 2 illustrates the difference between methods 1 and 2. Consider the M-cone data (green). The template fit to the full spectrum in panel A was achieved with a sum of 30% A1 and 70% A2. The λ_{max} values of the components are unrealistic (and not used for any further analysis); they emerge only as collaterals to the characterization of the shape of the spectrum by a sum of DLH-coupled template pairs without prior constraints on λ_{max}(A1) or λ_{max}(A2). Most importantly, the data points around the actual peak of the spectrum play no role in template-fitting other than defining the amplitude of the spectrum. In Fig. 2A, this is illustrated by the two other curves (violet, pure A1 template; orange, pure A2 template), which have been set to have the same λ_{max} (543.4 nm) and peak value (here normalized to unity) as the best-fitting template, yet fail conspicuously in reproducing most of the spectrum. By contrast, method 2 is defined to take into account only the data points around peak. Fig. 2B illustrates least-square parabola fits to data ±30 nm around peak of the same recordings as in panel A. This gives the value 547 nm for the cone peak, not so different from the 543.4 nm of the template fit. (The correlation of λ_{max} values as determined by the two types of fits for all individuals is shown in Fig. 4A,B.)

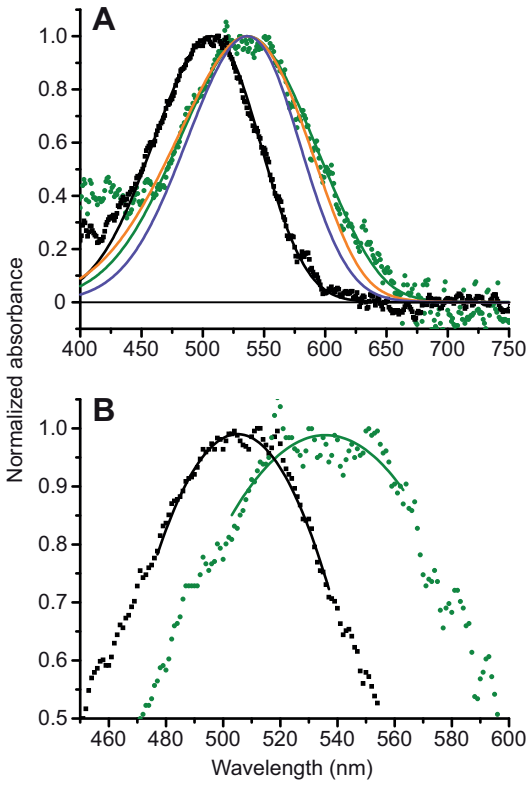

Fig. 2. Comparison of template and parabola fits as methods for estimating different chromophore ratios in rods (black) and M-cones (green). The data are averages of recordings from 28 rods and 15 M-cones in the same individual (from PYO2011). (A) Judged by template-fitting to the full spectra, rod λ_{max}=508 nm and cone λ_{max}=543.4 nm. The black curve is the template for a pure (100%) A1 pigment with λ_{max}=508 nm; the green curve is the template for 30% A1 with λ_{max}(A1)=522 nm and 70% A2 with λ_{max}(A2)=559 nm. The two dashed curves are templates for pure A1 (violet) and pure A2 (orange), both with λ_{max}=543.4 nm. (B) Judged by parabola-fitting to the domain around peak, rod λ_{max}=506 nm and cone λ_{max}=547 nm, indicating that rods have 81–92% A1 and cones have 0% A1 (i.e. pure A2) according to the assumptions explained in the Materials and methods.

Method 3: principal component analysis of mixed pigment spectra

Splitting the total variance into a number of principal components (1st, 2nd, 3rd, etc.) is a standard method in chemistry and bioinformatics. With PCA it is possible, for example, to separate spectra of different molecules present in a population of samples (e.g. Ward et al., 2003; Mäkelä et al., 2011). In work related to visual science, this approach has been used, for example, for analysis of natural illumination spectra (Judd et al., 1964) and plumage reflectance of birds (Cuthill et al., 1999). Interpretation of PCA results is not easy, however, as variation components identified purely statistically do not necessarily bear any close relation to real-world components. We still wanted to include the PCA analysis, as we think it does offer additional insight (see Table 1 and Discussion) and holds promise as a novel technique in the context of visual pigments.

We performed PCA at the population level, including in each analysis all single-cell rod or M-cone spectra recorded in the population in question. The spectra analyzed comprised 441 data points (HEL2011, RYT2011 and PYO2011), 405 data points (MAS) or 373 data points (all other 2008 spectra). The analyses included between 57 and 172 single-cell spectra for both cell types, depending on the population. Pooling all cells from a population in one analysis will of course conceal variation between individuals, but we did not have enough data to run the analysis at the level of individuals. The components were plotted and primary component graphs with clear peaks were recognized. The exact wavelengths of component peaks were determined by least-square fitting of second-order polynomials to points ±50 nm around a provisional peak estimate.

Light measurement

The spectral distribution of downwelling light (quanta m^{-2} s^{-1} nm^{-1} between 400 and 750 nm) was measured with a QSM 2500 submersible quantum spectrometer (Techtum, Umeå, Sweden) (see Lindström, 2000). Measurements were taken in full daylight in September 2011 between 11:00 and 15:00 h, from the water surface all the way to the bottom in the habitats HEL, ISO, RYT and PYO at 1–5 m intervals. The spectral properties of the four other habitats were estimated by visual comparison with these and a highly red-shifted lake (Tuusulanjärvi) measured by Jokela-Määttä et al. (Jokela-Määttä et al., 2007). At least two scans were taken at each depth. One scan of the full wavelength range took approximately 1 min.

RESULTS

DNA sequencing: no amino acid difference in the rod opsin between populations

The rod opsin gene was sequenced in three specimens of each population and translated into the corresponding amino acid sequence to look for changes in the protein part of the visual pigment. A BLAST search indicated that the 856-bp DNA sequences obtained showed the highest DNA and amino acid homologies (97% in each) with the rhodopsin gene from the three-spined stickleback (*Gasterosteus aculeatus*). No DNA sequence differences were

found among the 24 individuals studied, with the exception of two individuals (one from HEL and the other from MAS), which had one heterozygous synonymous change (GenBank accession no. JQ619638). Protein properties derived from sequencing of genomic DNA may in principle be subject to uncertainty because of potential differences in the transcribed products, but such variation has not been described for visual opsins. If opsins are identical, all spectral variation in the rod visual pigment must be due to varying proportions of chromophores A1 and A2. Consistent with this, the range of spectral variation in rods approximately coincided with the λ_{max} range defined by the DLH relationship for pure A1 and pure A2 chromophore in the same opsin (see Materials and methods).

MSP: four spectral classes of cones and cone opsins

In six of the eight populations studied, at least three spectral classes of cones (S, M and L) were found in addition to rods (Fig. 3). The exceptions are WHI and MAS, where no L-cones were recorded. Although a true loss shared by these two populations, which have been separated for less than a century (see Materials and methods), cannot be ruled out, it is likely that the apparent lack of L-cones is a bleaching artefact. These two populations are A2-dominated (Table 1), and the A2 version of the L-cone pigment absorbs strongly in the transmission band (>650 nm) of the edge filter used during preparation in 2008 (cf. Fig. 3B). In 2011, when we used infrared light, we did not, unfortunately, have access to specimens from these two populations.

Most of the λ_{max} variation within each of the initially delimited classes S, M and L could be explained by differing proportions of chromophores A1 and A2 (see below). However, the S-cone spectra averaged within individuals formed two non-overlapping clusters, with λ_{max} ranges of 407–412 and 426–458 nm, respectively. The dispersion of λ_{max} within clusters can be partly correlated with variation in chromophore content, as the A2 versions even of S-pigments are shifted towards longer wavelengths compared with their A1 counterparts. Hárosi's (Hárosi, 1994) formula predicts that a pigment with λ_{max}(A1)=407 nm should have λ_{max}(A2)=414 nm, which is roughly consistent with the width of the short-wavelength cluster. The 32 nm width of the long-wavelength cluster is somewhat surprising, however, as only a ca. 7 nm (Hárosi, 1994) or 12 nm (Whitmore and Bowmaker, 1989) difference between the A1 and A2 versions is predicted for pigments around 430 nm. It should be observed, however, that the cluster width refers to variation between individuals across all populations (including variation due to the low quality of many individual S-cone spectra). The population extremes for S-cones in the long-wave cluster (means ± s.e.m.) were 432.1±2.6 nm (PYO2011, N=4) and 448.3±2.3 nm (MAS, N=6). The experimental range is statistically significantly larger than the A1–A2 difference predicted by Hárosi (7 nm, P<0.05) (Hárosi, 1994), but not significantly larger than that predicted by Whitmore and Bowmaker (12 nm) (Whitmore and Bowmaker, 1989).

There is little doubt that the two clusters represent two different opsins, possibly SWS1 (giving 'violet' pigments at 355–440 nm) and SWS2 (giving 'blue' pigments at 410–490 nm) (cf. Yokoyama and Yokoyama, 2000; Hofmann and Carleton, 2009). Because of the limited material, we have no clear picture of the coexistence of SWS1 and SWS2 cones at the individual level, but all three populations studied in 2011 had both types. In 2008, recordings were obtained only from the longer-wavelength type of S-cone.

In L-cones, the population means of λ_{max} ranged from 550 nm (PYO2011) to 606 nm (HEL2011). The DLH prediction for λ_{max}(A1)=550 nm is λ_{max}(A2)=607 nm, and thus the extremes of the population means are consistent with nearly pure A1 and A2 in a

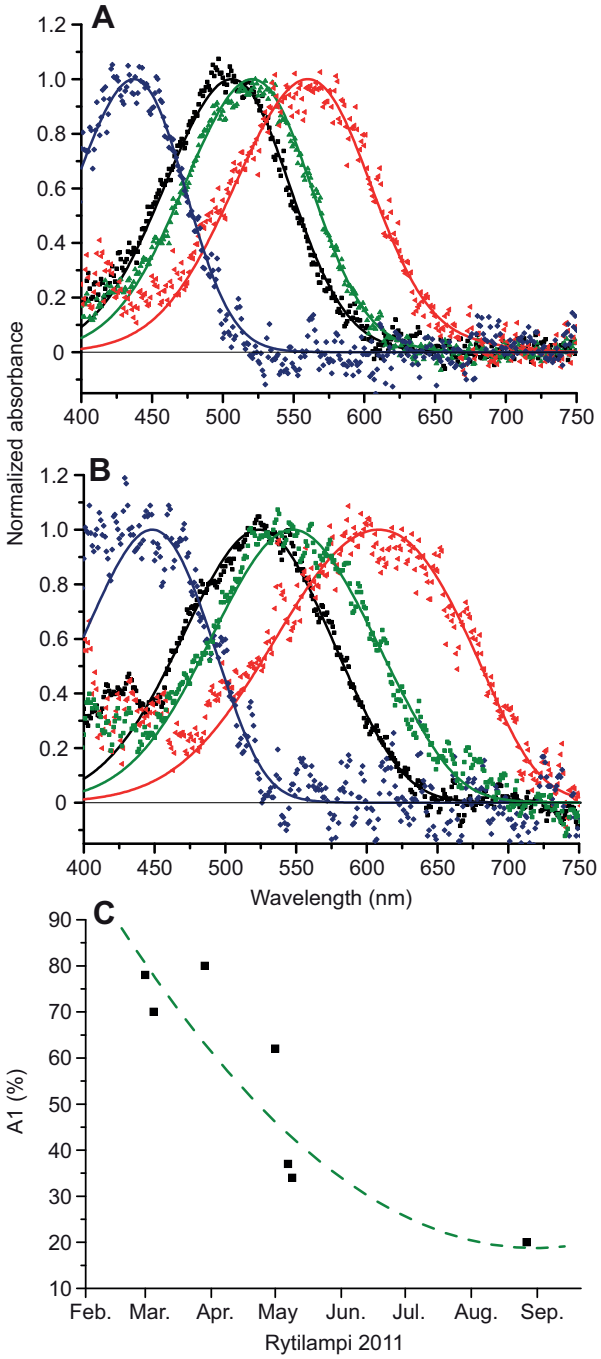

Fig. 3. (A,B) Spectra of four photoreceptor types as recorded in two individuals: one where the rods had nearly pure A1 pigment (A), and one with strongly A2-dominated rods (B). Both individuals are from the RYT population, recorded in March 2008 (A) and in May 2011 (B). All spectra have been normalized to peak absorbance 1. The curves are mixed A1–A2 templates of Govardovskii et al. (Govardovskii et al., 2000), giving the following λ_{max} values: (A) rods (black, λ_{max}=506 nm; number of cells averaged n=31), S-cones (blue, λ_{max}=437 nm, n=4), M-cones (green, λ_{max}=521 nm, n=24) and L-cones (red, λ_{max}=560 nm, n=20); (B) rods (black, λ_{max}=524 nm, n=23), S-cones (blue, λ_{max}=448 nm, n=8), M-cones (green, λ_{max}=545 nm, n=9) and L-cones (red, λ_{max}=608 nm, n=20). (C) Change in chromophore ratio of rods in the RYT population in 2011. The ordinate shows A1 percentages estimated by template-fitting to individual mean rod spectra in March (N=2), April (N=1), May (N=3) and September (N=2). The curve is a least-square parabola fitted to the points. Two individuals studied in September gave exactly the same value (20%) and therefore appear as a single point in the figure.

single opsin. For M-cones, the range of λ_{max} population means was 519–544 nm, well encompassed by the DLH relationship and thus consistent with a single opsin. However, the 25 nm range is so narrow that only one (or neither) of the boundaries can represent a pure-chromophore version of the pigment (see Materials and methods and below).

In conclusion, our MSP data suggest that the nine-spined stickleback has four classes of cone opsins expressed in four classes of cone outer segments. The L-cone outer segments recorded were most often members of M–L double cones. There were no indications that the complements of cone opsins differ between the eight populations investigated. Spectral variation within each cone class was consistent with varying chromophore proportions in a single opsin (with a cautionary reservation for the longer-wavelength S-cone).

Varying chromophore proportions in rods and cones

The populations fell into two distinct groups (hereafter referred to as groups 1 and 2) with respect to mean rod λ_{max}. In group 1, comprising populations with A1-dominated rods (Table 1, data sets 1–5), population means of rod λ_{max} were in the range of 505–511 nm. In group 2, comprising populations with A2-dominated rods (Table 1, data sets 6–10), population means of rod λ_{max} were in the range of 527–529 nm. Fig. 3 shows representative spectra of rods and cones from an A1-dominated individual (panel A) and an A2-dominated individual (panel B). High A2 in rods correlated with high A2 in cones: all spectra shown in Fig. 3B are shifted towards longer wavelengths compared with those shown in Fig. 3A.

Our procedures were designed to minimize possible variation due to seasonal and/or developmental regulation of chromophore proportions. We studied only fully developed fish that had been kept for at least 6 months in aquaria at constant temperature (15°C) under a standardized light regime (see Materials and methods). Recordings were limited to January–May for the six main populations (WHI and MAS being exceptions). Under these conditions, A1(%) was generally a sufficiently stable characteristic to allow meaningful comparisons between populations.

In only one data set (RYT2011) was a clear seasonal change between January and May observed (Fig. 3C). In fact, the data shown in Fig. 3A,B are both from RYT individuals, but recorded in different seasons: the spectra in panel A (rod λ_{max}=506 nm) were recorded in March 2008, those in panel B (rod λ_{max}=524 nm) in May 2011. In RYT2011, rod λ_{max} drifted from 510 nm in mid-March (n=2), through ca. 523.5 nm in mid-May (n=3) to 527 nm in extra recordings made in early September (n=2) especially to study this question. On the one hand, this proves that the nine-spined stickleback as a species does have the capacity to regulate chromophore proportions, although we do not know the factors that govern the shifts. On the other hand, and most importantly, none of the other data sets in our material showed a systematic shift of λ_{max} in the time window of our recordings (supplementary material Fig. S1). The properties of populations and the contrasts between them were also constant enough across the years 2008 and 2011 to support meaningful comparisons between populations (Table 1). This does not, of course, mean that there could not be chromophore changes in some or all of these populations at other times or under other conditions.

From Fig. 3A,B as well as similar sets of spectra recorded from individuals of the other populations (supplementary material Fig. S2) it is finally evident that S- and L-cone spectra tended to be of lower quality than rod and M-cone spectra because of noisier recordings and/or smaller numbers of cells recorded. The main rod/cone comparisons were therefore based on M-cones.

Quantitative estimation of chromophore proportions in rods and M-cones

Fig. 4 plots λ_{max} and A1(%) for rods and M-cones as obtained by the two independent methods of analysis, with the results of method 1 on the abscissa and those of method 2 on the ordinate. Fig. 4A,B shows the λ_{max} values for each individual fish from which a sufficient number of single-cell spectra were obtained, different populations being distinguished by different symbols. There is fair agreement between values obtained by the two methods (method 1, r^2=0.966 for rods and 0.933 for M-cones; method 2, r^2=1.008 for rods and 0.951 for M-cones). In the rod data (panel A), the segregation into a short-wavelength group 1 and a long-wavelength group 2 is immediately evident, whereas the distribution of M-cone λ_{max} is less clearly bimodal.

Fig. 4C,D correspondingly relates population-level estimates of A1(%) according to methods 1 and 2. In the rod data, the segregation of group 1 (A1-dominated, upper right cluster) and group 2 (A2-dominated, lower left cluster) is again obvious, except for one outlier (WHI, green star in Fig. 4C). This deviant data point reflects the fact that method 1, when applied to very noisy data (poorly defined spectral shape), is not good at disentangling the two fitting parameters λ_{max}(A1) and A1(%) (see Materials and methods). Thus, for WHI rods the (unconstrained) best fit was achieved with mean λ_{max}(A1)=520 nm, giving A1(%)≈80%. Fitting the same data under the constraint λ_{max}(A1)=504.8 nm (the lowest rod population mean) gives mean A1(%)=22%; however, several of the individual spectra are then poorly fitted even by the pure A2 template (0% A1). Although the latter strategy might have been a reasonable alternative when fitting rod spectra, as the opsin was known to be the same in all populations, we chose not to do so in order to preserve the independence of methods 1 and 2 and to analyze rods and M-cones in the same way. It is worth noting that this problem, the trade-off of λ_{max} and A1:A2 in fitting, is encountered whenever 'mixed' spectra are analyzed without prior knowledge of the components, for example, when studying a new species.

As previously pointed out, method 2 is not susceptible to this type of error. Instead, it requires a prior assumption regarding the λ_{max} of the pure components, and is sensitive to the accuracy of that assumption (to which method 1 is immune). In Fig. 4C,D, 45 deg lines that would correspond to perfect correlation of values obtained by the two methods have been drawn for visual guidance; the obvious deviations are indicative of their different error sources. Yet the correlation is good enough to make it meaningful to average them to yield a single final estimate for A1(%) in each data set (Table 1, Fig. 5).

Fig. 5 summarizes the A1(%) of rods and M-cones for each of the data sets. The estimates from methods 1 and 2 were averaged for each individual, and the bars in the histogram give means ± s.d. of (arcsine-transformed) individual estimates. The rod–cone differences within data sets were tested by two-way ANOVA (photoreceptor type; data set) on the arcsine-transformed values. The rod–cone differences in chromophore proportions were statistically significant for all data sets in group 1 and for none of those in group 2 (at the P<0.05 level, i.e. satisfying the criterion P<0.0045 prior to Bonferroni correction for n=11).

Method 3: decomposing mixed spectra by principal component analysis

For PCA, all single-cell spectra (either from rods or from M-cones) were pooled within each population. It should be realized that PCA gives variance fractions explained by spectral components that are identified on purely statistical grounds, not measures of

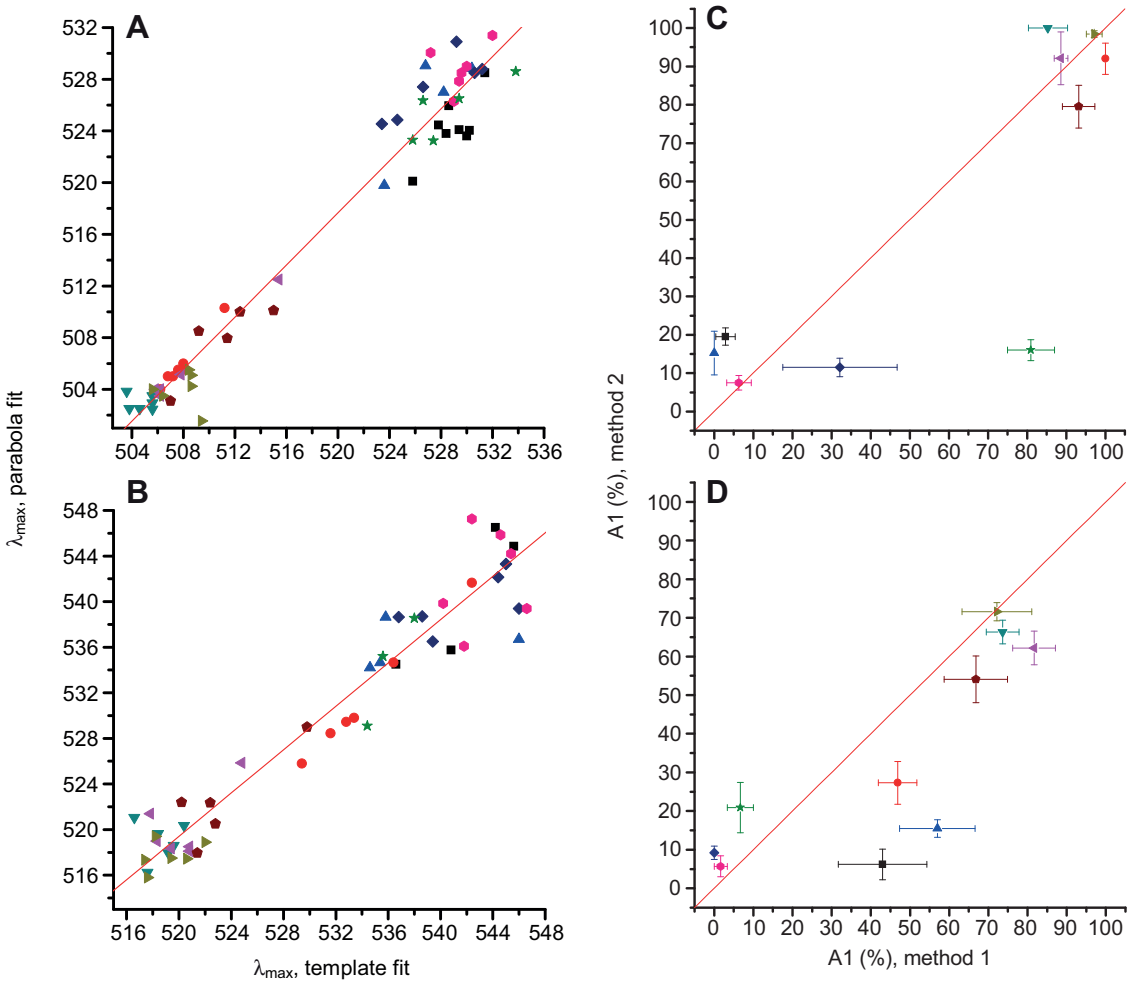

Fig. 4. (A,B). Estimates of λ_{max} of rods (A) and cones (B) obtained by fitting Govardovskii et al. (Govardovskii et al., 2000) templates (abscissa) and parabolas (ordinates) to spectra of individual fish. Each symbol type indicates one data set as follows (enumerated in the same order as in Table 1): Group 1: ABB2008 (green triangle pointing to the right), ISO2008 (brown pentagon), PYO2008 (turquoise inverted triangle), PYO2011 (red circle), RYT2008 (pink triangle pointing to the left); Group 2: BOL2008 (blue diamond), HEL2008 (blue upright triangle), HEL2011 (black square), WHI2008 (green star), MAS2008 (pink hexagon). The equations of the least-square lines fitted to the data are: (A) rods, y=1.008x+6.324 (r^2=0.966); (B) cones, y=0.951x+24.964 (r^2=0.934). (C,D) Estimates of A1(%) of rods (C) and cones (D) obtained by method 1 (abscissa) and method 2 (ordinates); data are means ± s.d. for each data set. Symbols for the data sets as in A and B. The lines are 45 deg lines drawn for visual guidance. See Materials and methods and Results for details.

chromophore proportions. Thus PCA components need not correspond to real visual-pigment spectra. Yet if there is little variation in chromophore proportions between cells, the primary PCA component is usually close to the main peak (α-band) of the recorded spectrum (capturing variation in absolute amplitude between recorded spectra). In contrast, if the chromophore proportions vary between cells, this is liable to emerge as a PCA component resembling the A1–A2 difference spectrum. Because there are many factors causing variation in recorded spectra, however, even the variance of recordings from a single homogeneous visual pigment (with a single chromophore) may emerge as consisting of several rather similar PCA components. It was common in our analysis to obtain two visual-pigment-like PCA components that differed only in the β-band domain, although the peak was in the α-band. To make Table 1 more readable, we excluded components explaining a lower percentage of the variance if there was another component within 10 nm that explained a higher percentage. With this qualification, Table 1 shows the peak wavelengths of all major PCA components ('major' defined as explaining at least 1% of the total variance), and the percent of the total variance explained by each.

For ABB, BOL and MAS (data sets 1, 6 and 10), PCA analysis had little to add, as the only major component found in rods as well as cones was similar to the full recorded spectrum. Several of the others, however, merit comment. The A1–A2 difference spectra of Govardovskii et al. (Govardovskii et al., 2000) templates for λ_{max}(A1)=504.8 nm (rods) and λ_{max}(A1)=512.5 nm (M-cones) have broad peaks at 530–610 nm (maximum at 568 nm) and 540–630 nm (maximum 579 nm), respectively. In the ISO and the RYT2011 data sets (nos 2 and 11), the second principal components in rods and cones are consistent with these. Intriguingly, RYT2008 (data set 5) also has a rod component suggestive of the A1–A2 difference spectrum. This may signal an incipient rod chromophore switch in the RYT population also in the year 2008 (like in 2011), detected by PCA, although still too small to be detected as a λ_{max} shift or a significant change in spectral shape.

The components identified by PCA in this data set are illustrated in Fig. 6. It is also the only case where PCA found a greater number

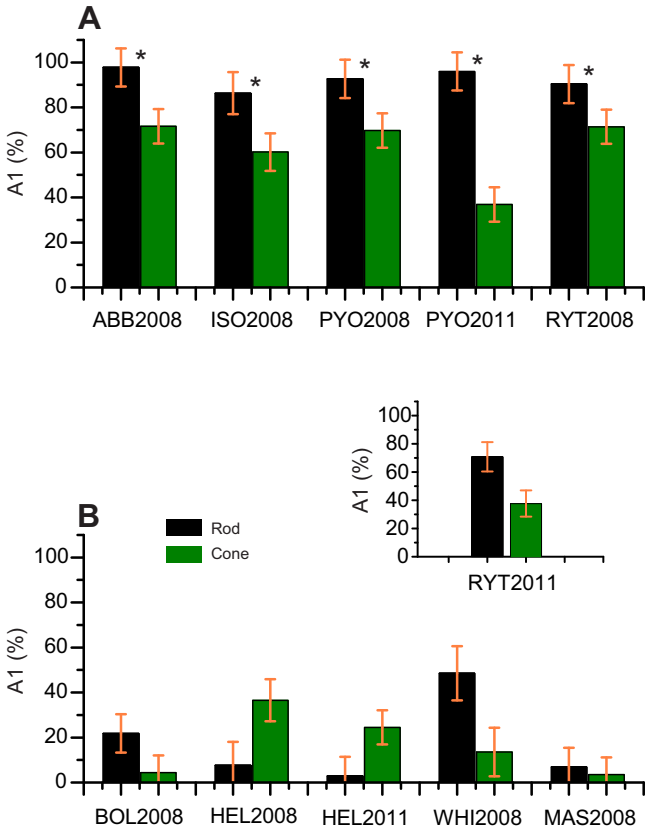

Fig. 5. A1 percentages of rods (black bars) and M-cones (green bars) in populations of group 1 (A), group 2 (B), and the data set RYT2011 reflecting a non-stationary situation (inset). Stars indicate rod–cone differences that are statistically significant at the $P<0.05$ level (observing the Bonferroni correction for non-independent testing of 11 data sets: $P=0.05/11=0.0045$). In group 1, all differences were significant ($P<0.0012$). In group 2, only WHI2008 was marginally significant ($P=0.0054$); for all others, $P>0.015$. Error bars are ±s.d. for the arcsine-transformed data.

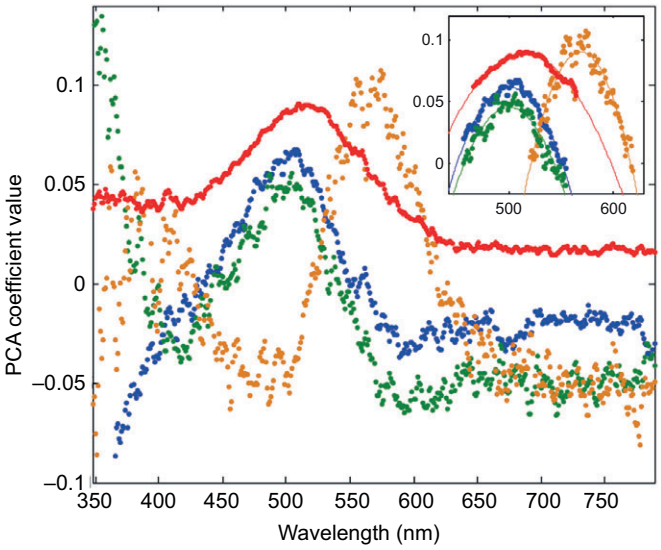

Fig. 6. Determination and interpretation of the principal variance components of a mixed spectrum. The full spectrum was that of rods in the data set RYT2008 (no. 5 in Table 1), peaking at ca. 507 nm. The first variance component (red curve, explaining 66.8% of the variance) is roughly congruent with the full spectrum. The next two components both peaking near 501 nm (blue and green curves, explaining 13.5 and 5.4%, respectively) are consistent with the pure A1 rod pigment. The fourth variance component, peaking at ca. 561 nm (yellow curve, explaining 2.1%), may be attributed to the A1–A2 difference spectrum. All other components explained less than 1% of the total variance and were therefore neglected (see Materials and methods and Results for details). Components 1, 2 and 4 have been inverted for the figure. The inset shows how the peak wavelengths of the component spectra were determined by least-square fitting of parabolas over the top.

of major variance components in rods than in cones (the cone PCA in the same data set gives the full pigment spectrum as the only major component).

The results for data set PYO2011 (no. 4 in Table 1) are also interesting, as M-cones yielded no less than four major PCA components. The first one (peaking at 532.5 nm) simply represents the full spectrum. The two following ones (519.8 and 546.8 nm) resemble the spectra of the pure chromophore components, and the last one (589.5 nm) is consistent with the M-cone A1–A2 difference spectrum. Rod spectra yieled two PCA components, which may be associated with the full spectrum and the rod A1–A2 difference spectrum, respectively (507.2 and 574.2 nm).

Chromophore proportions may be different in L- and M-cones

Our recordings from other cone types are not extensive enough to support comprehensive comparisons of chromophore proportions across populations. About the two classes of S-cones we can only say that their A1:A2 ratios varied, quite possibly over the full range from 0% to 100% A1 (see above). The L-cone data, however, do allow some definite conclusions, despite the fact that we have to limit ourselves to the 2011 recordings, as only they can be regarded as spectrally unbiased. They comprised one population from group 2 (HEL2011) and two from group 1 (PYO2011 plus the labile RYT2011). We based the analysis of chromophore proportions in L-cones on method 2, as the observed population extremes of λ_{max} were consistent with those expected for an A1–A2 pair [λ_{max}(A1)≈550 nm and λ_{max}(A2)≈607 nm, see above].

The results from PYO2011, the only stable group 1 data set among these, are the most interesting. Mean λ_{max} in L-cones was 550.3±1.9 nm ($N=7$, $n=133$). This corresponds to 100% A1, congruent with the rods, whereas the M-cones of the same individuals were estimated to have only 40% A1 (see Fig. 5A, Table 1). The L–M difference in A1(%) is statistically significant (two-tailed $P<0.001$ on a t-test for paired, arcsine-transformed values).

The group 2 data set HEL2011 conforms to the notion that A2 dominance in rods correlates with A2 dominance in all cone types (cf. Fig. 3). Population mean λ_{max} of L-cones was 606.4±3.7 nm ($N=5$, $n=20$), indicating practically 0% A1 (compare with an estimated 3% in rods and 27% in M-cones of the same data set). Fig. 7 shows the population-mean spectra of M-cones and L-cones of PYO2011 (panel A) and HEL2011 (panel B).

As previously mentioned, RYT2011 was in a state of transition. Individual mean values of L-cone λ_{max} went from ca. 548 nm in March ($N=2$, $n=12$) to ca. 602 nm in May ($N=2$, $n=21$). The corresponding A1 percentages would be 100 and 9%, respectively, suggesting a switch even more complete than in the rods (which went from 76 to 32% A1; see Fig. 3C).

DISCUSSION

Differences in rod absorbance spectra are due to variable chromophore ratios

DNA sequencing revealed no amino acid variation in the rod opsin gene. Thus variation in λ_{max} of the rod visual pigment must be due

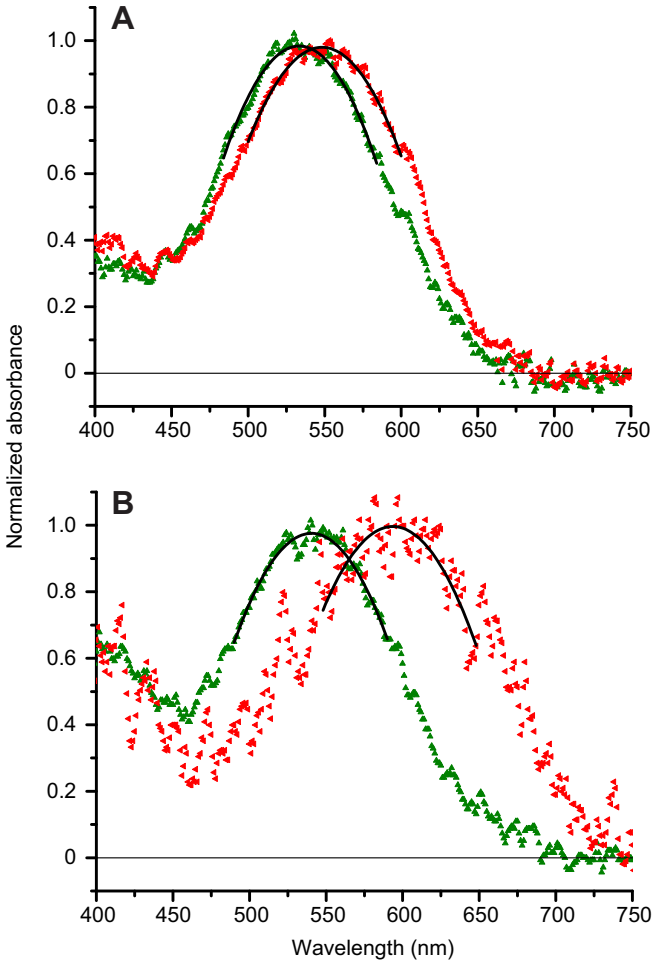

Fig. 7. Comparison of M-cone (green) and L-cone (red) spectra averaged across all individuals in two of the data sets. (A) Group 1 population PYO (no. 4 in Table 1), with estimated A1(%)≈40% for M-cones and 100% for L-cones (both based on fits to spectra of the same seven individuals). The spectra have been fitted with parabolas ±50 nm around a provisional peak; these give λ_{max}≈533 nm (M) and 549 nm (L). (B) Group 2 population HEL (no. 8 in Table 1), with estimated A1(%)≈23% for M-cones and 0% for L-cones (the latter based on fits to spectra of five individuals). The parabola fits shown indicate λ_{max}≈541nm (M-cones) and 596 nm (L-cones). Note that these λ_{max} values estimated from the population-level average spectra deviate slightly from those calculated as means of the λ_{max} values obtained by separate fitting of each individual spectrum in the same data set (i.e. the values given in the Discussion and Table 1).

to varying proportions of chromophores A1 and A2. Consistent with this, the observed variation range of rod λ_{max} closely matched the DLH prediction for a visual pigment that has a λ_{max} of ~504 nm when coupled to the A1 chromophore.

The populations fell into two distinct groups differing with respect to λ_{max} and the dominant chromophore of the rod pigment: short-wavelength-sensitive, A1-dominated (group 1) and long-wavelength-sensitive, A2-dominated (group 2; see Table 1, Fig. 5). Reinvestigation of three populations (PYO, RYT from group 1 and HEL from group 2) after a 3 year interval indicated that the differences were quite robust over the years for fish that had been kept under the same standardized conditions and studied at approximately the same time of the year. The differences invite a simple generalization based on habitat type. Group 1 consists of populations from freshwater habitats cut off from the sea thousands of years ago (Donner, 1995; Eronen et al., 2001). Group 2 consists of salt- or brackish-water populations plus a population from Mashinnoye pond, which has been separated from the sea for a few decades only (see Materials and methods). This apparent sea/lake dichotomy was unexpected and may be due to chance, as it resulted from a sample of only eight populations.

At least three points should be noted when judging this result. First, as indicated by RYT2011 (Fig. 3C), the nine-spined stickleback (like many other fishes) possesses the capacity to regulate the chromophore content of visual pigments on a physiological time scale, although the factors that govern the balance in this species are unknown. The spectral 'snapshots' considered here certainly do not give a full picture of how chromophore proportions in freshwater and brackish-water populations may change under natural conditions. Second, the fish from all populations were kept in freshwater aquaria under similar conditions for several months before experiments, and the same saline was used for all retinas during preparation and recording. Thus there cannot have been differential effects of ions directly on the visual pigment. Third, the common generalization that sea and lake fishes differ with respect to chromophore usage goes in the opposite direction (our sea populations have more A2 chromophore and the lake populations have more A1 chromophore, which is against the general trend) (Wald, 1937; Wald, 1939; Bridges, 1972; Jokela-Määttä et al., 2007; but see Wald, 1941; Schwanzara, 1967), which generally makes more sense, as spectral transmission in lakes tends to be red-shifted (which would favour A2) compared with that in seas (Jerlov, 1976).

Even though they cannot at present be given a clear ecological interpretation, the differences between groups 1 and 2 indicate genetic differences (with the possible exceptions of WHI and MAS, which were studied in a different season than the other populations). These may have to do with norms of reaction to some environmental factors, intrinsic seasonal rhythms or the degree of plasticity in chromophore proportions. We do not know, but we can make theoretical predictions about the relative performance of A1 and A2 versions of the pigments in their present light environments (see below).

Four spectral classes of cones

We found four spectral classes of cones, each consistent with one of the four main classes of cone opsin genes in the vertebrate lineage (*SWS1*, *SWS2*, *RH2* and *M/LWS*) (cf. Yokoyama and Yokoyama, 2000; Hofmann and Carleton, 2009). Our failure to find one or the other of the cone classes in some populations was most probably due to bleaching (in L-cones) or mere chance (for S-cones), and cannot be taken to suggest that populations differ in their cone complements.

The ranges of λ_{max} variation within each of the four cone classes, as well as the shapes of spectra as analyzed in M-cones, were consistent with the idea that the only tuning mechanism was the varying proportions of chromophores A1 and A2. Thus we analyzed the cone spectra, like the rod spectra, on the assumption that the opsins did not differ between populations.

Different chromophore proportions in rods, M-cones and L-cones

The most interesting discovery was that all populations in group 1 had a significantly higher fraction of A2 chromophore in the M-cones than in the rods. Mechanistically, this might be implemented by the recently described delivery of 11-*cis* chromophore to cones from Müller cells (Wang et al., 2009; Wang and Kefalov, 2011). This makes cones partly independent of the retinal pigment

epithelium, previously thought to be the only source for all photoreceptors (Fain et al., 1996; cf. Reuter et al., 1971). Functionally, the privileged supply of 11-*cis* chromophore to cones has been interpreted as a means of ensuring fast and reliable regeneration of cone pigment without competition with rods (e.g. Suzuki et al., 1985). In the present study, it also emerges as a potential way of achieving independent spectral tuning of rod and cone visual pigments. For this to work, one must assume independently regulated A1 to A2 conversion (by a regulated retinol 3,4-dehydrogenase) somewhere *en route* to the visual pigment in the cone outer-segment membranes. Chromophore selectivity could also be due to cone-specific mechanisms (cone-specific localization of the dehydrogenase, or 11-*cis* transport or uptake). Any mechanistic scheme must remain speculative at this stage, and would also have to accommodate the fact that L-cones can differ from M-cones in chromophore content. Selective chromophore handling by different types of rods is known from several species of deep-sea fish (Bowmaker et al., 1988; Crescitelli, 1989).

Our conclusions are based on A1:A2 estimation by two independent methods, which gave essentially concurrent results (Fig. 4), whereas their potential error sources were mainly different (cf. Materials and methods). The only assumption common to both that could potentially introduce correlated bias is the coupling of λ_{max}(A1) and λ_{max}(A2) of pigment pairs by the Hárosi (Hárosi, 1994) relationship. Alternative and slightly different coupling relationships have been proposed previously (Whitmore and Bowmaker, 1989; Parry and Bowmaker, 2000). All of these are purely phenomenological descriptions of certain data sets, of which the set used by Hárosi (Hárosi, 1994) is the most extensive. Moreover, in the wavelength domain critical for stickleback rods and M-cones [λ_{max}(A1) between 500 and 520 nm], the Hárosi predictions for λ_{max}(A2) are rather precisely intermediate between those of the two others. The maximal difference in predicted λ_{max}(A2) in this domain is ±5 nm, which would slightly change our A1:A2 estimates, but by too little to be of any significance for the conclusions. Around L-cone λ_{max}(A1) (≈550 nm), the Hárosi and Whitmore–Bowmaker relationships give practically identical predictions, whereas λ_{max}(A2) according to the Parry–Bowmaker relationship is lower by more than 5 nm in this domain. The difference would not significantly affect the comparison of A1(%) in M- and L-cones, however.

The performance of A1 and A2 rods and cones in the light environments of the sticklebacks

Rods

'Optimal' performance of a visual pigment depends on what is assumed to be its main task. For rod pigments, the benchmark often adopted is absolute visual sensitivity. This requires maximizing the SNR in very dim light, where the dominant noise is 'dark noise', intrinsic to the visual neurons, rather than noise arising from the Poisson fluctuations of the photon flux (Barlow, 1956). In rods of many species, the main intrinsic noise component liable to interfere with light detection comes from randomly occurring spontaneous (thermal) activations of visual-pigment molecules (Baylor et al., 1980; Aho et al., 1988; Ala-Laurila et al., 2004a; Luo et al., 2011). Maximizing the SNR then requires not only that the visual pigment catch photons efficiently, but also that it be thermally stable. Because the rate of thermal activation of visual pigments correlates strongly with red sensitivity (Luo et al., 2011), optimization of a pigment for light environments rich in long wavelengths faces an intricate trade-off. The advantage of a red-shift that increases quantum catch (QC) in a certain environment may be offset or even reversed in terms of SNR by the associated increase in thermal noise. Increasing noise is an inevitable correlate when red-tuning is achieved by an A1 to A2 chromophore switch in the same opsin (Donner et al., 1990; Ala-Laurila et al., 2004b; Ala-Laurila et al., 2007), whereas red-tuning by opsin changes may combine spectrally relevant amino acid substitutions with other (thermally relevant) amino acid substitutions that mitigate the decrease in thermal stability (Fyhrquist et al., 1998; Koskelainen et al., 2000).

However, the main goal for rod vision need not always be to maximize absolute sensitivity, but to support good vision at slightly higher (still scotopic) light levels. From some mean luminance upwards, photon fluctuations will surpass thermal activation as the main source of pigment-originated noise even in photoreceptors with 'noisy' pigments. Above that level, spectral tuning for increased QC will always increase SNR. (The critical light level in itself will, of course, depend on the noisiness of the pigment.) This idea has been invoked to explain general rod/cone differences (Barlow, 1957; Lythgoe, 1984), but may also be applied to variation in rod properties.

Fig. 8A shows a family of spectra (normalized to unity at peak) describing the downwelling light at different depths in one of the habitats, HEL, measured in daylight in September 2011 (see Materials and methods). The spectra (peaking around 570 nm) are quite representative of all except one (ABB) of the habitats in the present study. Other spectra measured at the same time were ISO (peak transmission at ca. 575 nm), RYT (565 nm) and PYO (565 nm). The four remaining habitats were not measured, but BOL, WHI and MAS appeared similar to the others as judged by eye. The only obvious outlier is ABB, a humic pond with strongly red-shifted transmittance.

The vertical lines in Fig. 8 mark λ_{max} of the pure A1 (violet) and pure A2 (orange) versions of the rod pigment. Two points are worth noting. First, regardless of chromophore, rod absorbance spectra are positioned at far too short wavelengths to make efficient use of the available light under most illuminations (except maybe under the blue skylight at dusk or dawn), a well-known situation in coastal and freshwater fish species (Lythgoe, 1979; Lythgoe, 1984). Second, 100% A2 chromophore would provide the best spectral match of the rod pigment to the downwelling light in all the water bodies of the present study. Why, then, do not all eight populations use A2 in rods? The most reasonable explanation is the noisiness of A2 pigments.

Jokela-Määttä et al. (Jokela-Määttä et al., 2007) have calculated relative QC (QC_{rel}) and conceptual SNR at the absolute threshold (SNR_{dark}) of A1 and A2 visual pigments as functions of λ_{max} for five different aquatic environments, some of which are very similar to the ones used in the present study, and summarized the results in graphic form (their fig. 3). Calculation of QC is straightforward (convolution of pigment absorptance spectra with illumination spectra). For calculation of SNR_{dark} it may be assumed that the frequency of thermal pigment activations is a monotonically increasing function of λ_{max}, $F(\lambda_{max})$, as modelled by Ala-Laurila et al. (Ala-Laurila et al., 2004a) and essentially confirmed by Luo et al. (Luo et al., 2011). The noise intrinsic to the visual pigment is proportional to the standard deviation of Poisson-distributed thermal 'dark' events within some integration time t_i. Because the Poisson standard deviation is equal to the square root of the mean (relative), SNR_{dark} may be defined as:

$$SNR_{dark} = QC_{rel} / \sqrt{[F(\lambda_{max}) \times t_i]} . \quad (1)$$

As only relative values interest us here, the integration time t_i may be used as an arbitrary proportionality constant. SNR_{dark} is a relevant measure of pigment performance at the very lowest light levels, where thermal activations dominate over photon fluctuations as a source of pigment-originated noise. Estimates of QC_{rel} and

SNR_{dark} for the A1 and A2 versions of stickleback rod pigment in the present habitats (excepting ABB) can be interpolated from two of the curve sets in Jokela-Määttä et al. (Jokela-Määttä et al., 2007),

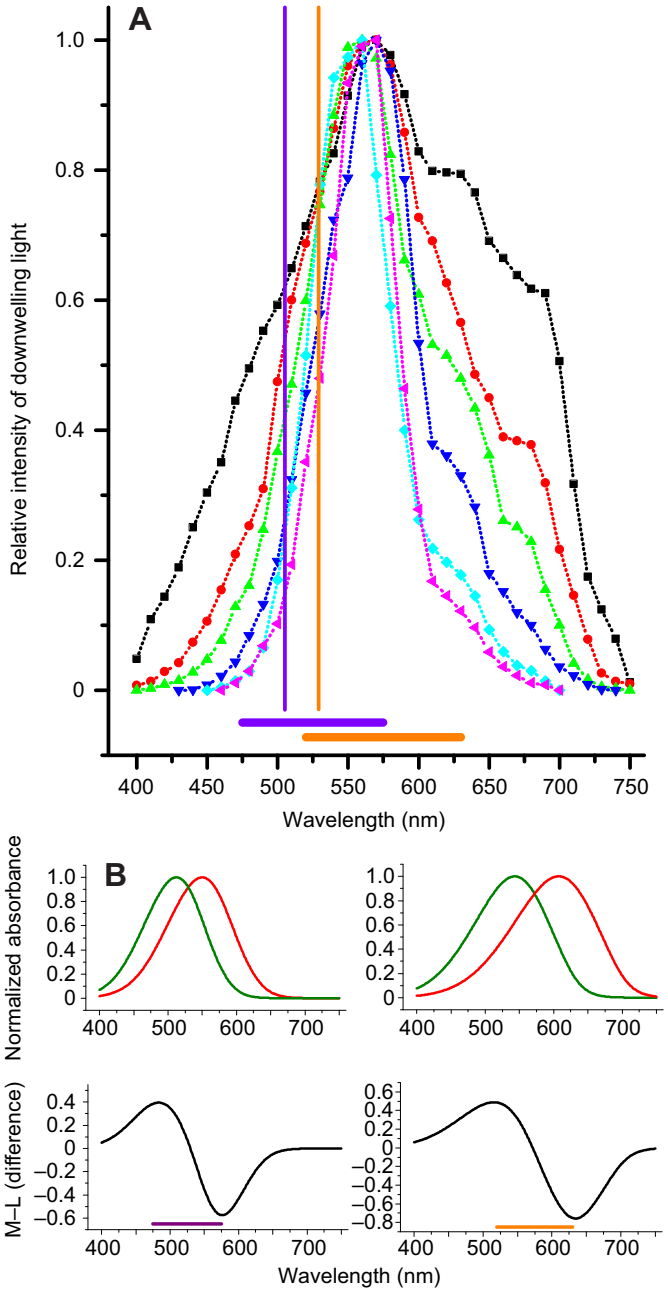

Fig. 8. Visual pigments with A2 chromophore provide better matches to the present light environments of the sticklebacks than those with A1 chromophore. The spectral distribution of downwelling light at different depths in the habitat HEL (representative of all the habitats except the red-shifted ABB) is here compared with rod λ_{max} (vertical lines: violet, A1; orange, A2), and domains of good wavelength discrimination as derived from by the M–L cone difference spectrum (horizontal bars: violet, A1; orange, A2). (A) The curve family gives spectra of downwelling light (quanta per unit area and unit time, relative units) measured in daytime in September 2011 at depths of 1 (broadest spectrum), 2, 3, 5, 8 and 9.4 m (narrowest spectrum). (B) How the domains of good wavelength discrimination are derived from M–L difference spectra. Top row: spectra of M-cones (green) and L-cones (red) with A1 (left) and A2 (right) chromophore. Bottom row: M–L difference spectra (black curves). The steep parts that correspond to domains of high wavelength resolution span ca. 475–575 nm for A1 (violet bar) and ca. 520–630 nm for A2 (orange bar).

which refer to light spectra peaking at 560 nm (their *B*) and 580 nm (their B_p), respectively. The estimates suggest that rods with the A2 chromophore would catch ca. 30% more quanta than those with the A1 chromophore on average in light environments like HEL (Fig. 8A). Judged by SNR_{dark}, the relationship is reversed: at the absolute threshold, A1 rods would perform more than 50% better than A2 rods on average. An ultra-adaptationist hypothesis might be that group 2 sticklebacks 'want to' see well at moderate scotopic light levels (and thus use A2), whereas group 1 fish 'want to' maximize absolute sensitivity (and thus use A1). (In humic lakes such as ABB, however, A2 would be superior in terms of both QC_{rel} and SNR_{dark}.) To evaluate this hypothesis, one would have to study the behaviour of the fish in their natural habitats in different seasons.

Cones

In brighter light, the disadvantages brought by the stronger 'dark noise' and lower photosensitivity of A2 compared with A1 pigments (cf. Dartnall, 1972; Bridges, 1972) are expected to matter much less. Hence, cones may have less reason than rods to avoid the A2 chromophore, and optimal chromophore proportions in a given light environment may be quite different for cones and rods. If the task is achromatic contrast discrimination by a single type of cone, QC is the relevant measure of pigment performance in brighter light. Estimates based on the modelling of Jokela-Määttä et al. (Jokela-Määttä et al., 2007) (see above) suggest that the A2 version of the M-cone pigment achieves 30% higher QC than its A1 counterpart in a light environment such as HEL (Fig. 8A). For the L-cone pigment, however, the A1 version remains superior, as $QC_{A1}/QC_{A2}=1.5$. Yet the L-cones of the local HEL population had nearly 100% A2 (see Results).

This apparent paradox is resolved, however, when the performance of L-cones is related to their main task, colour vision, where the elementary operation is wavelength discrimination by comparison of signals from M- and L-cones. Fig. 8B illustrates how a measure of wavelength discrimination based on subtractive coupling can be derived from M–L difference spectra. Discrimination is best in the domains where the M–L difference signal changes steeply as function of wavelength [i.e. the derivative $|d(M–L)/d\lambda|$ is large]. The main domains are marked by a violet bar for the A1 pigments and by an orange bar for the A2 pigments (these bars have been reproduced in panel A). On the whole, the M–L pair using A2 pigments is seen to match the light spectra much better than that using A1. A crucial factor is the protracted long-wavelength limb of the M-cone A2 pigment, which extends the upper bound of the domain of good discrimination from 575 to 630 nm. However, it must be remembered that the A1 to A2 switch will also red-shift the short-wave limb of the M-cone, which could in turn compromise wavelength discrimination at the interface with S-cones. A full analysis of M-cone performance in wavelength discrimination would have to observe the demands of both 'red–green' and 'yellow–blue' opponency, and a full functional description would have to be formulated in terms of the resultant colour space (e.g. Vorobyev and Osorio, 1998).

Here, however, we shall consider only one section through the complex discrimination space. Assume that A2 in M-cones is fixed at 100%. How does M–L discrimination change when the percentage of A2 in L-cones [denoted L(A2)] rises from 0 to 100%? In Fig. 9, the inset shows a family of M–L difference spectra at 10% intervals of L(A2). Besides the width of the discrimination domain, the crucial variable is the steepness of the difference spectrum within that domain [$|d(M–L)/d\lambda|$; see above], which defines resolving power. The steepness there is nearly constant and can be described by straight

lines. The slope coefficients β of these lines (suitably normalized) may be used as relative measures of wavelength discrimination. These have been plotted as functions of L(A2) in Fig. 9 (violet curve in the main panel), showing that wavelength resolution improves monotonically with increasing L(A2). This function would hold at high illumination levels, where photon fluctuations dominate over thermal pigment activations as a source of pigment-originated noise. At low light levels, however, the intrinsic noisiness of A2 pigments in general and L(A2) pigment in particular cannot be neglected, and in the limiting case, the thermal pigment activations are completely dominant compared with photoactivations. The thermal activation rate of the L-cone A2 pigment may be assumed to be some 50 times higher than that of either M-cone A2 or L-cone A1 pigments (cf. Ala-Laurila et al., 2004a; Ala-Laurila et al., 2007; Luo et al., 2011). Therefore, almost all (>90%) of the thermal activations liable to blur the M–L difference signal will be due to L(A2) pigment when its fraction of rises above some 20%, and the noisiness of the other pigments may be neglected. The (relative) wavelength discrimination function at the lowest light levels is then given by (cf. Eqn 1):

$$\mathrm{SNR}_{\mathrm{dark}} = C\beta / \sqrt{[\mathrm{L(A2)\%}]}, \quad (2)$$

where C is an arbitrary proportionality constant. Eqn 2 is plotted as the lower curve (blue) in Fig. 9, giving wavelength discrimination as function of A2 percentage in L-cones at very low light levels. Even then, there is significant improvement with increasing L(A2) at least up to 60–70%. As the mean light intensity increases, photon fluctuations gradually cause an increase in pigment-originated noise, and the 'operating function' will gradually shift from the blue to the violet curve. The main point of this example is to show that M–L wavelength discrimination may indeed benefit from high proportions of A2 in both M- and L-cones. In light environments where high absolute (scotopic) sensitivity requires high proportions of A1 in rods, there appear to be good functional reasons to use higher proportions of A2 in cones than in rods.

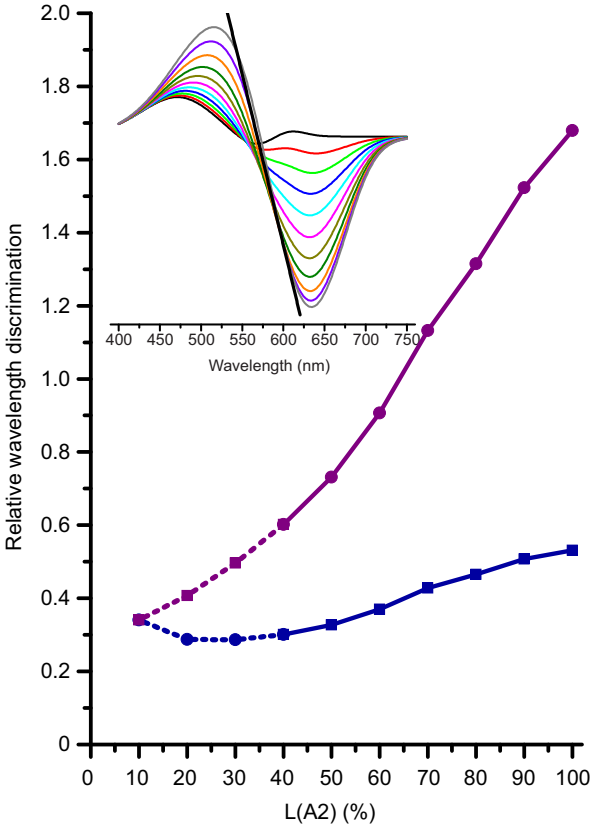

Fig. 9. Wavelength discrimination based on M–L cone difference spectra as a function of A2 percentage in the L pigment [L(A2)], when the M pigment is pure A2. The inset shows M–L difference spectra at 10% intervals of L(A2) (obtained as illustrated in Fig. 8B). The straight line exemplifies how the steepness of the slope is read from each curve. The slope coefficients are used as relative measures of wavelength resolution, plotted in the main graph (violet). However, below 40% L(A2), the discrimination domain gets narrower; this zone is marked by dashed lines. The square root of [L(A2)%/10] is taken as a relative measure of pigment 'dark' noise (see Discussion). When each slope coefficient is divided by this noise measure, a relative measure of the intrinsic SNR for wavelength discrimination is obtained [blue curve, anchored to the violet curve at 10% L(A2)]. The violet curve would describe the relationship in bright light, the blue curve at the lowest light levels.

Conclusions

Differences in visual-pigment absorptance spectra between eight populations of nine-spined stickleback were explained by differences in the proportions of chromophores A1 and A2. Within populations, chromophore proportions differed significantly between rods and M-cones, and between M-cones and L-cones. All populations with A1-dominated rods had significantly higher proportions of A2 in M-cones than in rods. Mechanistically, this indicates selective processing of 11-*cis* chromophore for different photoreceptor types. Functionally, higher A1 proportions in rods are consistent with a more compelling need to limit thermal noise, whereas higher A2 proportions in M-cones provide a better spectral match to prevailing light environments. The results suggest a possible ecological role for the different chromophore delivery pathways described recently.

ACKNOWLEDGEMENTS

We wish to thank Prof. David Hunt and Dr Wayne Davies for kindly providing the primer sequences and protocols for PCR, and Dr Magnus Lindström for help in measuring the spectra of downwelling light in the habitats. We are grateful for the skilful technical assistance of Dr Mirka Jokela-Määttä and Ms Sophie Aminoff.

FUNDING

This work was supported by the Academy of Finland [grant number 128081 to K.D. and numbers 129662 and 134728 to J.M.]; the Waldemar von Frenckell Foundation, The Societas Scientiarum Fennica and the Otto A. Malm Foundation [to J.P.]; and the University of Helsinki [to P.S.].

REFERENCES

Aho, A.-C., Donner, K., Hydén, C., Larsen, L. O. and Reuter, T. (1988). Low retinal noise in animals with low body temperature allows high visual sensitivity. *Nature* **334**, 348-350.

Ala-Laurila, P., Saarinen, P., Albert, R., Koskelainen, A. and Donner, K. (2002). Temperature effects on spectral properties of red and green rods in toad retina. *Vis. Neurosci.* **19**, 781-792.

Ala-Laurila, P., Donner, K. and Koskelainen, A. (2004a). Thermal activation and photoactivation of visual pigments. *Biophys. J.* **86**, 3653-3662.

Ala-Laurila, P., Pahlberg, J., Koskelainen, A. and Donner, K. (2004b). On the relation between the photoactivation energy and the absorbance spectrum of visual pigments. *Vision Res.* **44**, 2153-2158.

Ala-Laurila, P., Donner, K., Crouch, R. K. and Cornwall, M. C. (2007). Chromophore switch from 11-cis-dehydroretinal (A2) to 11-cis-retinal (A1) decreases dark noise in salamander red rods. *J. Physiol.* **585**, 57-74.

Archer, S., Hope, A. and Partridge, J. C. (1995). The molecular basis for the green-blue sensitivity shift in the rod visual pigments of the European eel. *Proc. R. Soc. B* **262**, 289-295.

Barlow, H. B. (1956). Retinal noise and absolute threshold. *J. Opt. Soc. Am.* **46**, 634-639.

Barlow, H. B. (1957). Purkinje shift and retinal noise. *Nature* **179**, 255-256.

Barlow, H. B. (1958). Temporal and spatial summation in human vision at different background intensities. *J. Physiol.* **141**, 337-350.

Baylor, D. A., Matthews, G. and Yau, K. W. (1980). Two components of electrical dark noise in toad retinal rod outer segments. *J. Physiol.* **309**, 591-621.

Beatty, D. D. (1975). Rhodopsin-porphyropsin changes in paired-pigment fishes. In *Vision in Fishes: New Approaches in Research* (ed. M. A. Ali), pp. 635-644. New York: Plenum Press.
Bowmaker, J. K., Dartnall, H. J. A. and Herring, P. J. (1988). Longwave-sensitive visual pigments in some deep-sea fishes: segregation of 'paired' rhodopsins and porphyropsins. *J. Comp. Physiol. A* **163**, 685-698.
Bridges, C. D. B. (1972). The rhodopsin-porphyropsin visual system. In *Handbook of Sensory Physiology VII/1: Photochemistry of Vision* (ed. H. J. A. Dartnall), pp. 417-480. Berlin: Springer-Verlag.
Browman, H. I. and Hawryshyn, C. W. (1994). The developmental trajectory of ultraviolet photosensitivity in rainbow trout is altered by thyroxine. *Vision Res.* **34**, 1397-1406.
Carleton, K. L. and Kocher, T. D. (2001). Cone opsin genes of african cichlid fishes: tuning spectral sensitivity by differential gene expression. *Mol. Biol. Evol.* **18**, 1540-1550.
Carlisle, D. B. and Denton, E. J. (1959). On the metamorphosis of the visual pigments of *Anguilla anguilla* (L.). *J. Mar. Biol. Assoc. UK* **38**, 97-102.
Crescitelli, F. (1989). The visual pigments of a deep-water malacosteid fish. *J. Mar. Biol. Assoc. UK* **69**, 43-51.
Cuthill, I. C., Bennett, A. T. D., Partridge, J. C. and Maier, E. J. (1999). Plumage reflectance and the objective assessment of avian sexual dichromatism. *Am. Nat.* **153**, 183-200.
Dartnall, H. J. A. (ed.) (1972). Photosensitivity. In *Handbook of Sensory Physiology*, Vol. VII/I, pp. 122-145. New York: Springer-Verlag.
Dartnall, H. J. A. and Lythgoe, J. N. (1965). The spectral clustering of visual pigments. *Vision Res.* **5**, 81-100.
Donner, J. (1995). *The Quaternary History of Scandinavia*. Cambridge: Cambridge University Press.
Donner, K., Firsov, M. L. and Govardovskii, V. I. (1990). The frequency of isomerization-like 'dark' events in rhodopsin and porphyropsin rods of the bull-frog retina. *J. Physiol.* **428**, 673-692.
Duan, W. and Fuerst, P. A. (2001). Isolation of a sex-linked DNA sequence in cranes. *J. Hered.* **92**, 392-397.
Eronen, M., Glückert, G., Hatakka, L., van de Plassche, O., van der Plicht, J. and Rantala, P. (2001). Rates of Holocene isostatic uplift and relative sea-level lowering of the Baltic in SW Finland based on studies of isolation contacts. *Boreas* **30**, 17-30.
Fain, G. L., Matthews, H. R. and Cornwall, M. C. (1996). Dark adaptation in vertebrate photoreceptors. *Trends Neurosci.* **19**, 502-507.
Fyhrquist, N., Donner, K., Hargrave, P. A., McDowell, J. H., Popp, M. P. and Smith, W. C. (1998). Rhodopsins from three frog and toad species: sequences and functional comparisons. *Exp. Eye Res.* **66**, 295-305.
Gonda, A., Herczeg, G. and Merilä, J. (2011). Population variation in brain size of nine-spined sticklebacks (*Pungitius pungitius*) – local adaptation or environmentally induced variation? *BMC Evol. Biol.* **11**, 75.
Govardovskii, V. I. and Zueva, L. V. (1988). A simple highly sensitive recording microspectrophotometer. *Tsitologiia* **30**, 499-502.
Govardovskii, V. I. and Zueva, L.V. (2000). Fast microspectrophotometer for studying the photolysis of visual pigments *in situ. Sensornye Sistemy* **14**, 288-296.
Govardovskii, V. I., Fyhrquist, N., Reuter, T., Kuzmin, D. G. and Donner, K. (2000). In search of the visual pigment template. *Vis. Neurosci.* **17**, 509-528.
Hargrave, P. A., McDowell, J. H., Curtis, D. R., Wang, J. K., Juszczak, E., Fong, S. L., Rao, J. K. and Argos, P. (1983). The structure of bovine rhodopsin. *Biophys. Struct. Mech.* **9**, 235-244.
Hárosi, F. I. (1994). An analysis of two spectral properties of vertebrate visual pigments. *Vision Res.* **34**, 1359-1367.
Herczeg, G. and Välimäki, K. (2011). Intraspecific variation in behaviour: effects of evolutionary history, ontogenetic experience and sex. *J. Evol. Biol.* **24**, 2434-2444.
Herczeg, G., Gonda, A. and Merilä, J. (2009a). Predation mediated population divergence in complex behaviour of nine-spined stickleback (*Pungitius pungitius*). *J. Evol. Biol.* **22**, 544-552.
Herczeg, G., Gonda, A. and Merilä, J. (2009b). Evolution of gigantism in nine-spined sticklebacks. *Evolution* **63**, 3190-3200.
Hofmann, C. M. and Carleton, K. L. (2009). Gene duplication and differential gene expression play an important role in the diversification of visual pigments in fish. *Integr. Comp. Biol.* **49**, 630-643.
Hope, A. J., Partridge, J. C. and Hayes, P. K. (1998). Switch in rod opsin gene expression in the European eel, *Anguilla anguilla* (L.). *Proc. R. Soc. B* **265**, 869-874.
Jerlov, N. G. (1976). *Marine Optics*. Amsterdam: Elsevier.
Jokela-Määttä, M., Pahlberg, J., Lindström, M., Zak, P. P., Porter, M., Ostrovsky, M. A., Cronin, T. W. and Donner, K. (2005). Visual pigment absorbance and spectral sensitivity of the *Mysis relicta* species group (Crustacea, Mysida) in different light environments. *J. Comp. Physiol. A* **191**, 1087-1097.
Jokela-Määttä, M., Smura, T., Aaltonen, A., Ala-Laurila, P. and Donner, K. (2007). Visual pigments of Baltic Sea fishes of marine and limnic origin. *Vis. Neurosci.* **24**, 389-398.
Jokela-Määttä, M., Vartio, A., Paulin, L. and Donner, K. (2009). Individual variation in rod absorbance spectra correlated with opsin gene polymorphism in sand goby (*Pomatoschistus minutus*). *J. Exp. Biol.* **212**, 3415-3421.
Judd, D. B., MacAdam, D. L., Wyszecki, G., Budde, H. W., Condit, H. R., Henderson, S. T. and Simonds, J. L. (1964). Spectral distribution of typical daylight as a function of correlated color temperature. *J. Opt. Soc. Am.* **54**, 1031-1040.
Koli, L. (1990). *Suomen Kalat*. Porvoo, Finland: Werner Söderström Osakeyhtiö.
Koskelainen, A., Ala-Laurila, P., Fyhrquist, N. and Donner, K. (2000). Measurement of thermal contribution to photoreceptor sensitivity. *Nature* **403**, 220-223.
Larmuseau, M. H., Raeymaekers, J. A., Ruddick, K. G., Van Houdt, J. K. and Volckaert, F. A. (2009). To see in different seas: spatial variation in the rhodopsin gene of the sand goby (*Pomatoschistus minutus*). *Mol. Ecol.* **18**, 4227-4239.
Larmuseau, M. H., Vancampenhout, K., Raeymaekers, J. A., Van Houdt, J. K. and Volckaert, F. A. (2010). Differential modes of selection on the rhodopsin gene in coastal Baltic and North Sea populations of the sand goby, *Pomatoschistus minutus*. *Mol. Ecol.* **19**, 2256-2268.
Lindström, M. (2000). Seasonal changes in the underwater light milieu in a Finnish Baltic sea coastal locality. *Geophysica* **36**, 215-232.
Luo, D. G., Xue, T. and Yau, K. W. (2008). How vision begins: an odyssey. *Proc. Natl. Acad. Sci. USA* **105**, 9855-9862.
Luo, D. G., Yue, W. W., Ala-Laurila, P. and Yau, K. W. (2011). Activation of visual pigments by light and heat. *Science* **332**, 1307-1312.
Lythgoe, J. N. (1979). *The Ecology of Vision*. Oxford: Clarendon Press.
Lythgoe, J. N. (1984). Visual pigments and environmental light. *Vision Res.* **24**, 1539-1550.
Mäkelä, A. V., Heikkilä, O., Kilpeläinen, I. and Heikkinen, S. (2011). ImatraNMR: novel software for batch integration and analysis of quantitative NMR spectra. *J. Magn. Reson.* **211**, 186-194.
Nathans, J. (1990a). Determinants of visual pigment absorbance: role of charged amino acids in the putative transmembrane segments. *Biochemistry* **29**, 937-942.
Nathans, J. (1990b). Determinants of visual pigment absorbance: identification of the retinylidene Schiff's base counterion in bovine rhodopsin. *Biochemistry* **29**, 9746-9752.
Parry, J. W. and Bowmaker, J. K. (2000). Visual pigment reconstitution in intact goldfish retina using synthetic retinaldehyde isomers. *Vision Res.* **40**, 2241-2247.
Parry, J. W., Carleton, K. L., Spady, T., Carboo, A., Hunt, D. M. and Bowmaker, J. K. (2005). Mix and match color vision: tuning spectral sensitivity by differential opsin gene expression in Lake Malawi cichlids. *Curr. Biol.* **15**, 1734-1739.
Reuter, T. (1969). Visual pigments and ganglion cell activity in the retinae of tadpoles and adult frogs (*Rana temporaria* L.). *Acta Zool. Fenn.* **122**, 1-64.
Reuter, T. E., White, R. H. and Wald, G. (1971). Rhodopsin and porphyropsin fields in the adult bullfrog retina. *J. Gen. Physiol.* **58**, 351-371.
Schwanzara, S. A. (1967). The visual pigments of freshwater fishes. *Vision Res.* **7**, 121-148.
Shand, J. (1993). Changes in the spectral absorption of cone visual pigments during the settlement of the goatfish *Upeneus tragula*: the loss of red sensitivity as a benthic existence begins. *J. Comp. Physiol. A* **173**, 115-121.
Shand, J., Hart, N. S., Thomas, N. and Partridge, J. C. (2002). Developmental changes in the cone visual pigments of black bream *Acanthopagrus butcheri*. *J. Exp. Biol.* **205**, 3661-3667.
Shikano, T., Shimada, Y., Herczeg, G. and Merilä, J. (2010). History vs. habitat type: explaining the genetic structure of European nine-spined stickleback (*Pungitius pungitius*) populations. *Mol. Ecol.* **19**, 1147-1161.
Spady, T. C., Seehausen, O., Loew, E. R., Jordan, R. C., Kocher, T. D. and Carleton, K. L. (2005). Adaptive molecular evolution in the opsin genes of rapidly speciating cichlid species. *Mol. Biol. Evol.* **22**, 1412-1422.
Spady, T. C., Parry, J. W., Robinson, P. R., Hunt, D. M., Bowmaker, J. K. and Carleton, K. L. (2006). Evolution of the cichlid visual palette through ontogenetic subfunctionalization of the opsin gene arrays. *Mol. Biol. Evol.* **23**, 1538-1547.
Suzuki, T., Makino-Tasaka, M. and Miyata, S. (1985). Competition between retinal and 3-dehydroretinal for opsin in the regeneration of visual pigment. *Vision Res.* **25**, 149-154.
Tamura, K., Peterson, D., Peterson, N., Stecher, G., Nei, M. and Kumar, S. (2011). MEGA5: molecular evolutionary genetics analysis using maximum likelihood, evolutionary distance, and maximum parsimony methods. *Mol. Biol. Evol.* **28**, 2731-2739.
Temple, S. E., Plate, E. M., Ramsden, S., Haimberger, T. J., Roth, W. M. and Hawryshyn, C. W. (2006). Seasonal cycle in vitamin A1/A2-based visual pigment composition during the life history of coho salmon (*Oncorhynchus kisutch*). *J. Comp. Physiol. A* **192**, 301-313.
Terai, Y., Seehausen, O., Sasaki, T., Takahashi, K., Mizoiri, S., Sugawara, T., Sato, T., Watanabe, M., Konijnendijk, N., Mrosso, H. D. et al. (2006). Divergent selection on opsins drives incipient speciation in Lake Victoria cichlids. *PLoS Biol.* **4**, e433.
Trokovic, N., Herczeg, G., Scott McCairns, R. J., Izza Ab Ghani, N. and Merilä, J. (2011). Intraspecific divergence in the lateral line system in the nine-spined stickleback (*Pungitius pungitius*). *J. Evol. Biol.* **24**, 1546-1558.
Vorobyev, M. and Osorio, D. (1998). Receptor noise as a determinant of colour thresholds. *Proc. Biol. Sci.* **265**, 351-358.
Vorobyev, M., Brandt, R., Peitsch, D., Laughlin, S. B. and Menzel, R. (2001a). Colour thresholds and receptor noise: behaviour and physiology compared. *Vision Res.* **41**, 639-653.
Vorobyev, M., Marshall, J., Osorio, D., Hempel de Ibarra, N. and Menzel, R. (2001b). Colourful objects through animal eyes. *Color Res. Appl.* **26 Suppl. 1**, S214-S217.
Wald, G. (1937). Visual purple system in freshwater fishes. *Nature* **139**, 1017-1018.
Wald, G. (1939). On the distribution of vitamins A_1 and A_2. *J. Gen. Physiol.* **22**, 391-415.
Wald, G. (1941). The visual system of euryhaline fishes. *J. Gen. Physiol.* **25**, 235-245.
Wald, G. (1946). The metamorphosis of visual system in Amphibia. *Biol. Bull.* **91**, 239.
Wang, J. S. and Kefalov, V. J. (2011). The cone-specific visual cycle. *Prog. Retin. Eye Res.* **30**, 115-128.
Wang, J. S., Estevez, M. E., Cornwall, M. C. and Kefalov, V. J. (2009). Intra-retinal visual cycle required for rapid and complete cone dark adaptation. *Nat. Neurosci.* **12**, 295-302.
Ward, J. L., Harris, C., Lewis, J. and Beale, M. H. (2003). Assessment of 1H NMR spectroscopy and multivariate analysis as a technique for metabolite fingerprinting of *Arabidopsis thaliana*. *Phytochemistry* **62**, 949-957.
Whitmore, A. V. and Bowmaker, J. K. (1989). Seasonal variation in cone sensitivity and short-wave absorbing visual pigments in the rudd *Scardinius erythrophthalmus*. *J. Comp. Physiol. A* **166**, 103-115.
Yokoyama, S. and Yokoyama, R. (2000). Comparative molecular biology of visual pigments. In *Handbook of Biological Physics*, Vol. 3: *Molecular Mechanisms in Visual Transduction* (ed. D. G. Stavenga, W. J. DeGrip and E. N. Pugh), pp. 257-296. Amsterdam: Elsevier.

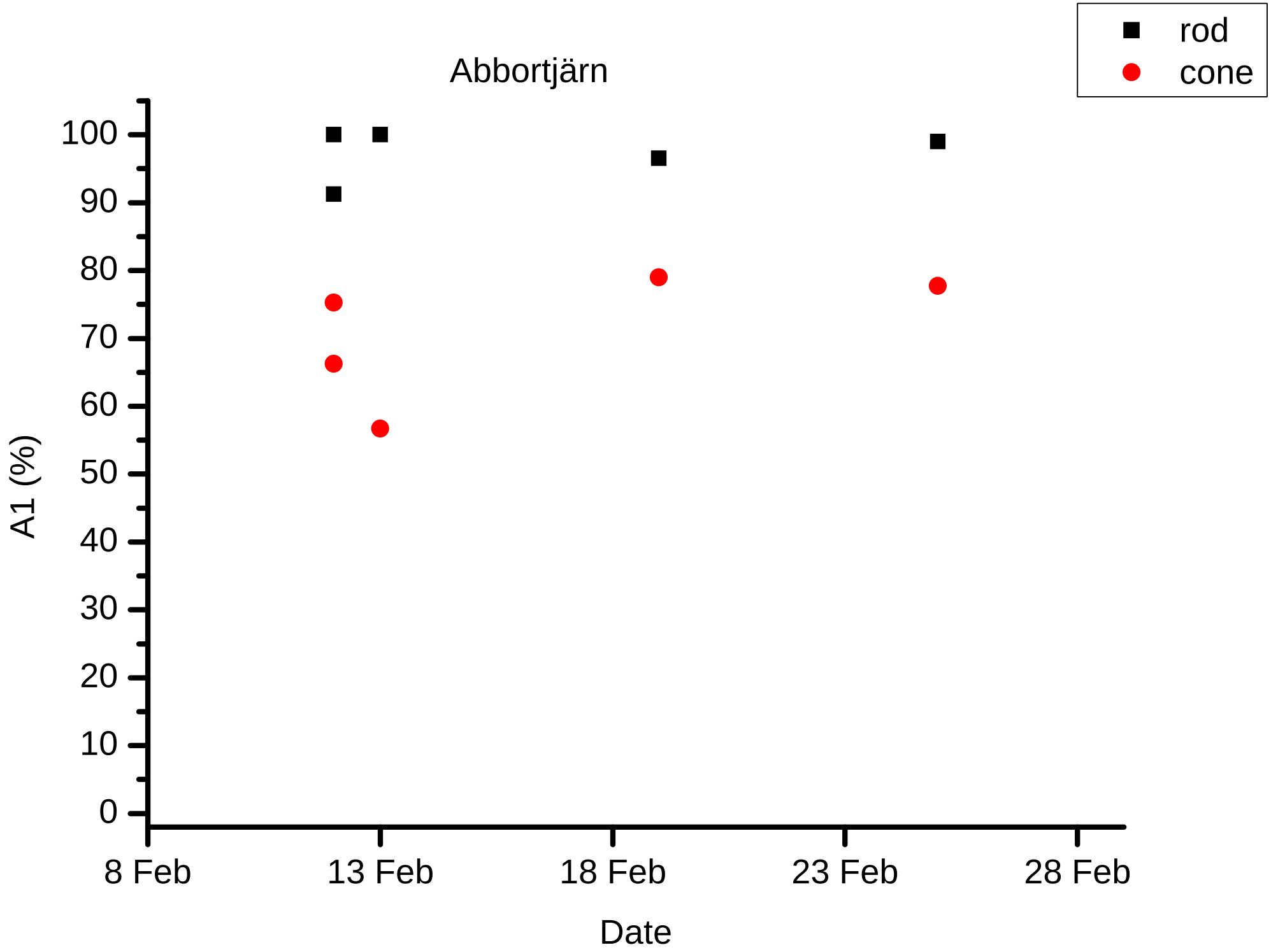
Abbortjärn
rod
cone
A1 (%)
100
90
80
70
60
50
40
30
20
10
0
8 Feb
13 Feb
18 Feb
23 Feb
28 Feb
Date

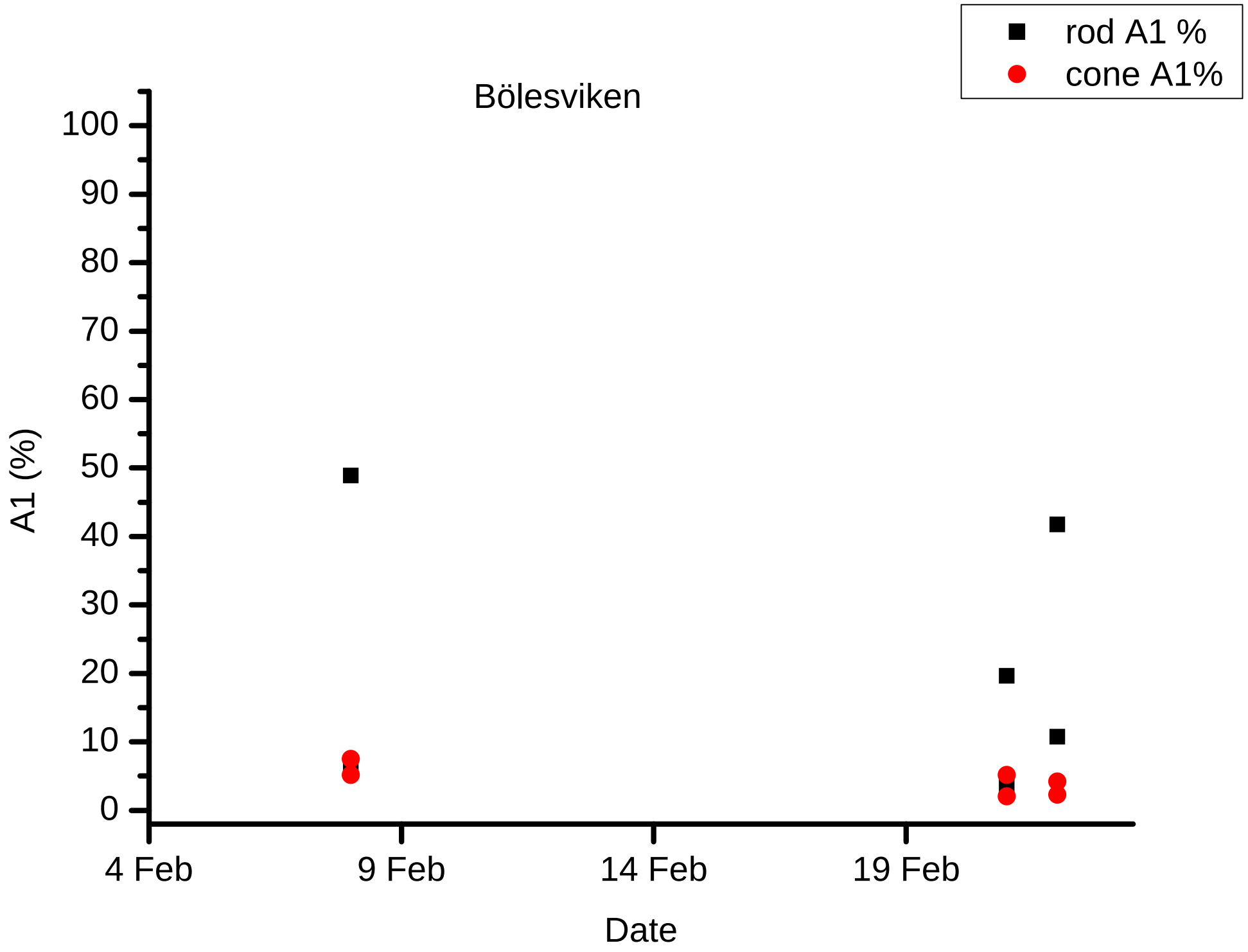
Bölesviken
rod A1 %
cone A1%
A1 (%)
100
90
80
70
60
50
40
30
20
10
0
4 Feb
9 Feb
14 Feb
19 Feb
Date

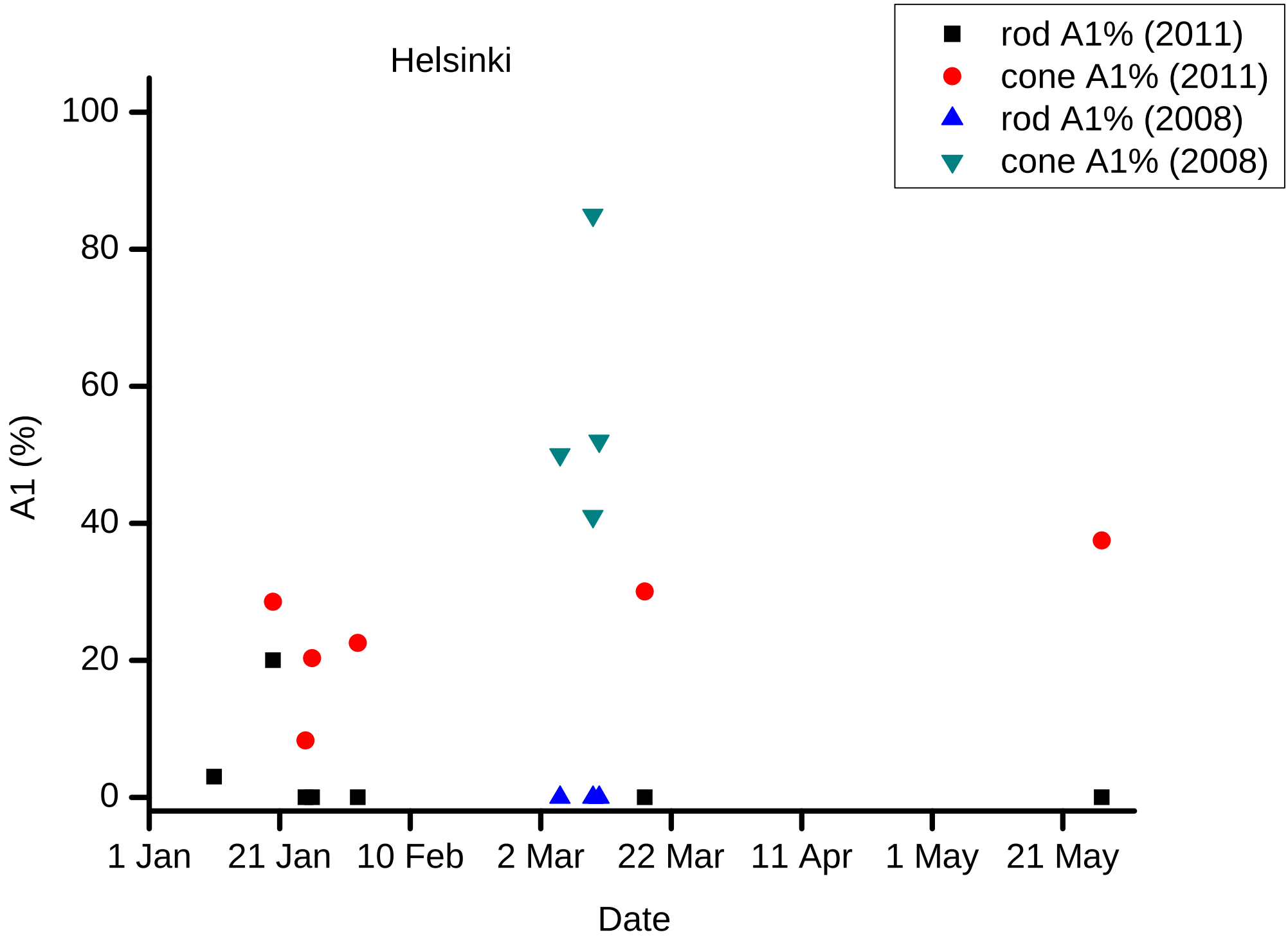
Helsinki
rod A1% (2011)
cone A1% (2011)
rod A1% (2008)
cone A1% (2008)
A1 (%)
100
80
60
40
20
0
1 Jan
21 Jan
10 Feb
2 Mar
22 Mar
11 Apr
1 May
21 May
Date

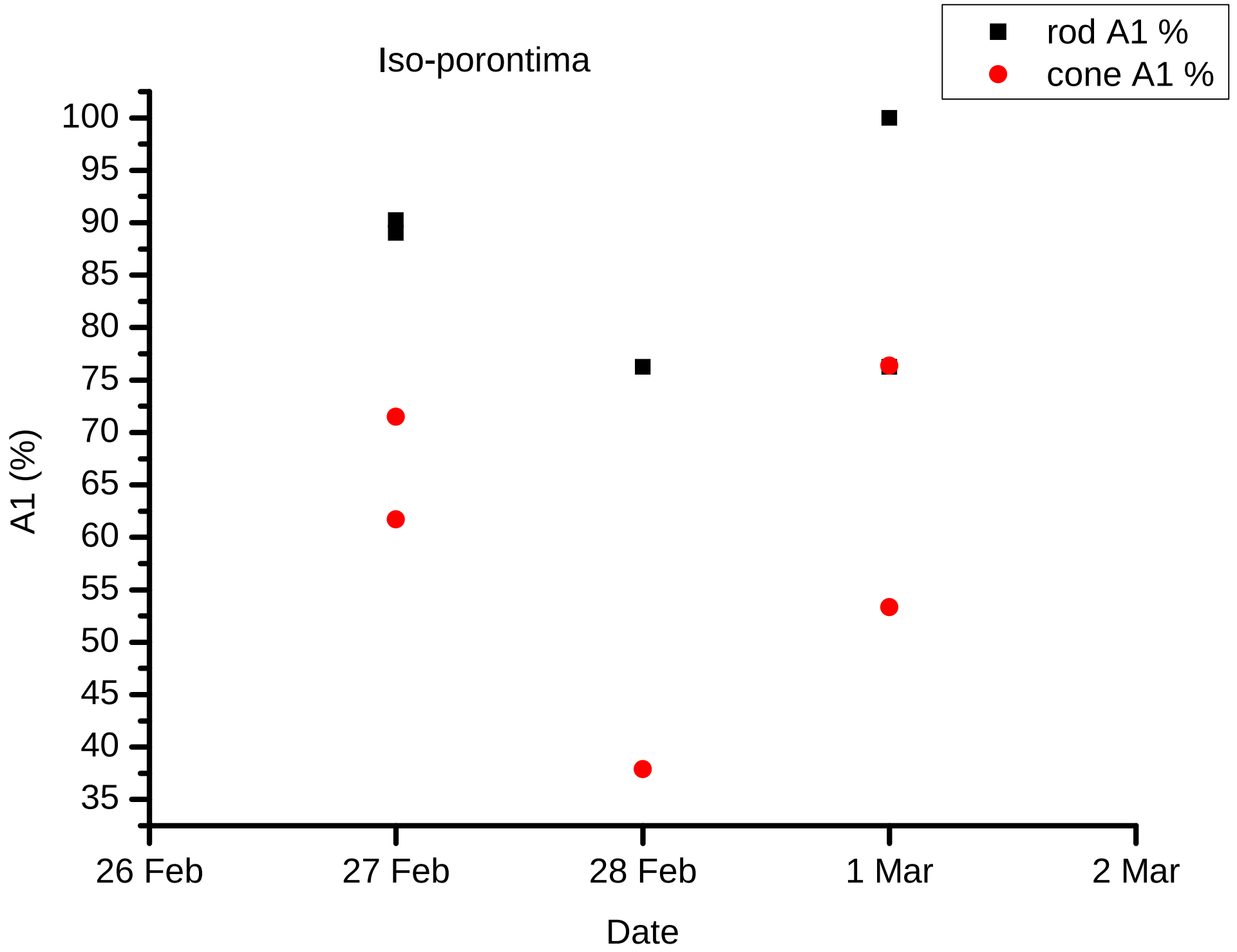
Iso-porontima
rod A1 %
cone A1 %
A1 (%)
100
95
90
85
80
75
70
65
60
55
50
45
40
35
26 Feb
27 Feb
28 Feb
1 Mar
2 Mar
Date

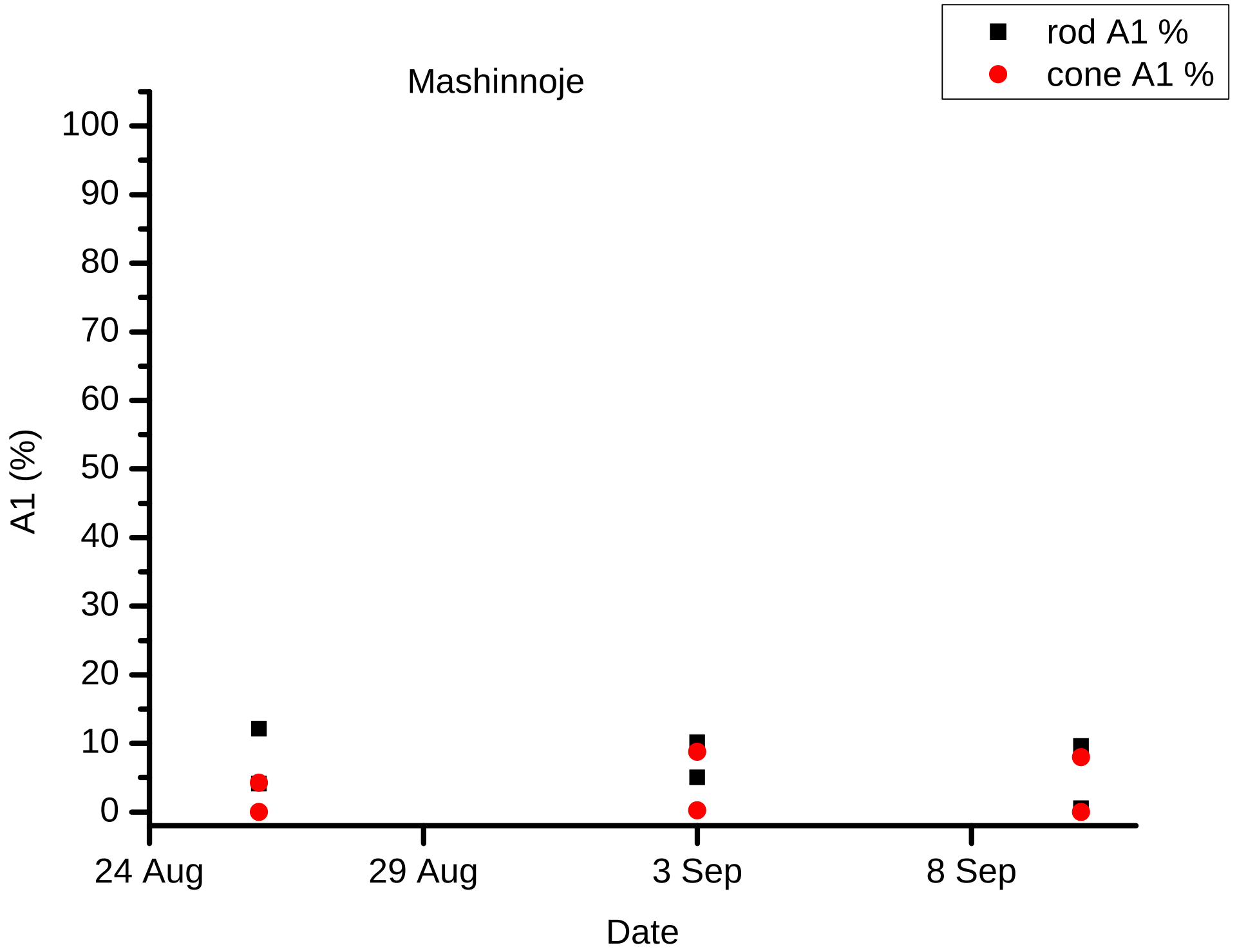
Mashinnoje
rod A1 %
cone A1 %
A1 (%)
100
90
80
70
60
50
40
30
20
10
0
24 Aug
29 Aug
3 Sep
8 Sep
Date

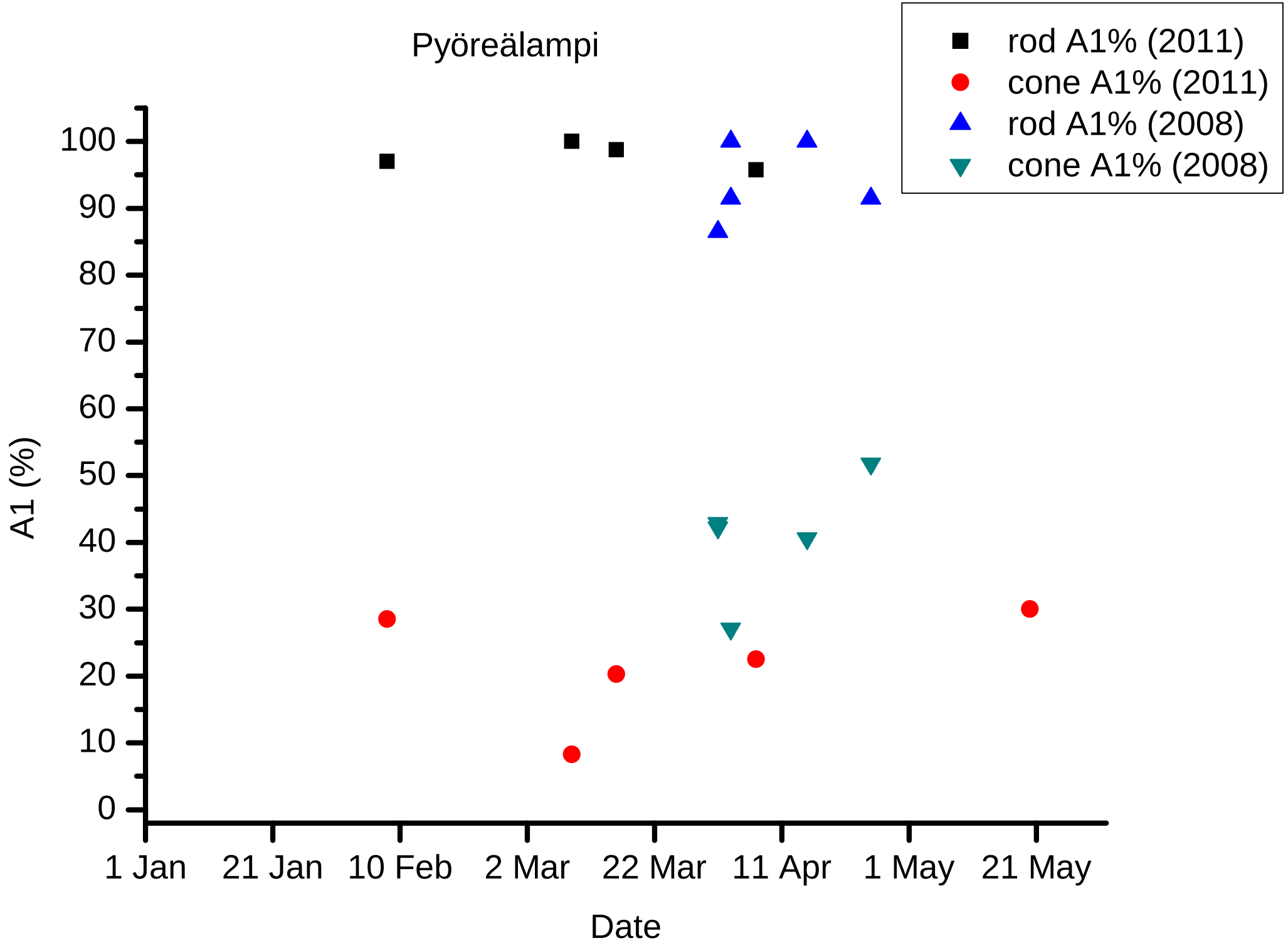
Pyöreälampi
rod A1% (2011)
cone A1% (2011)
rod A1% (2008)
cone A1% (2008)
A1 (%)
100
90
80
70
60
50
40
30
20
10
0
1 Jan
21 Jan
10 Feb
2 Mar
22 Mar
11 Apr
1 May
21 May
Date

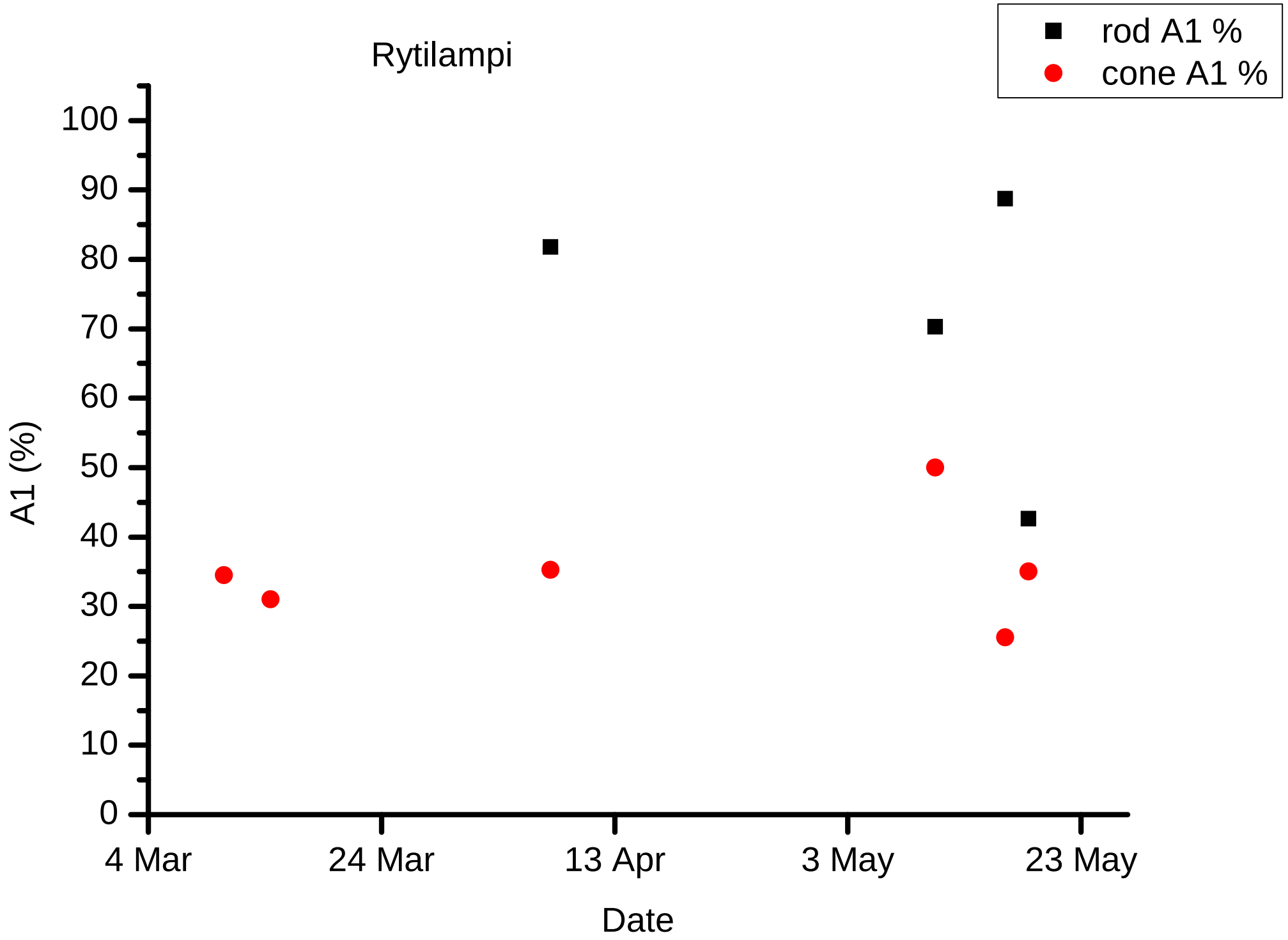
Rytilampi
rod A1 %
cone A1 %
A1 (%)
100
90
80
70
60
50
40
30
20
10
0
4 Mar
24 Mar
13 Apr
3 May
23 May
Date

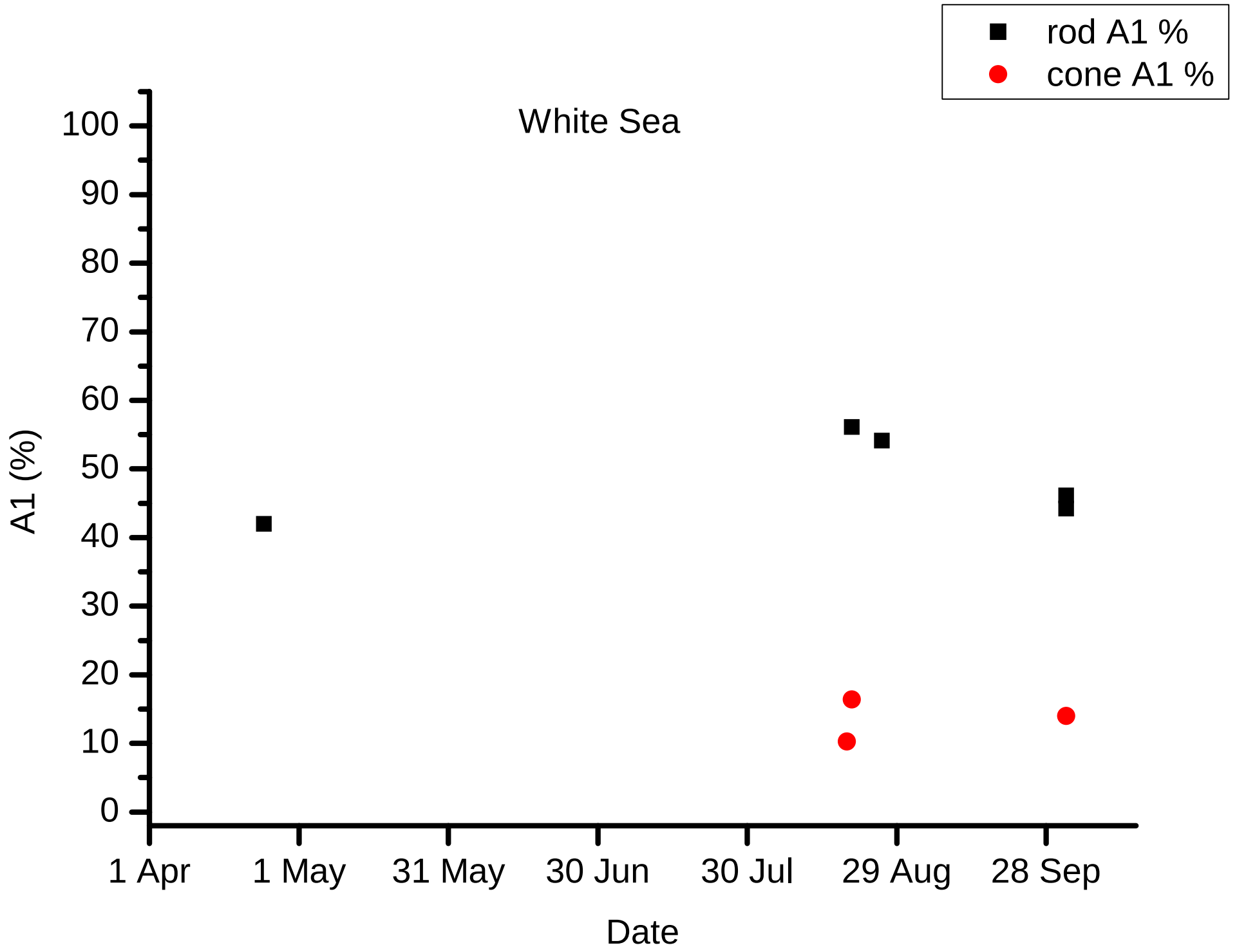
rod A1 %
cone A1 %
White Sea
A1 (%)
100
90
80
70
60
50
40
30
20
10
0
1 Apr
1 May
31 May
30 Jun
30 Jul
29 Aug
28 Sep
Date

25.2.2008a, Abbortjärn, *Pungitius pungitius*

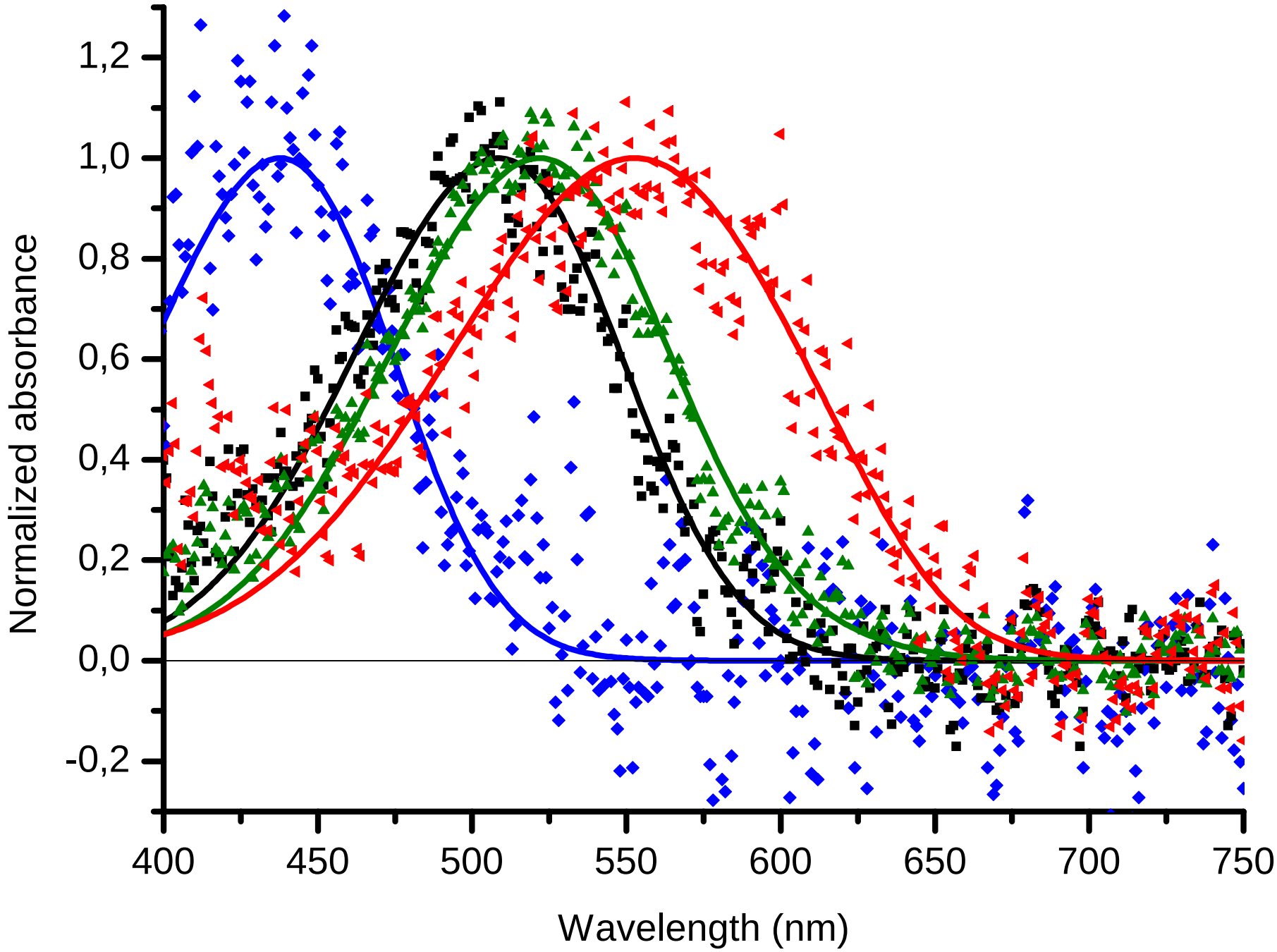

8.2.2008b, Bölesviken, *Pungitius pungitius*

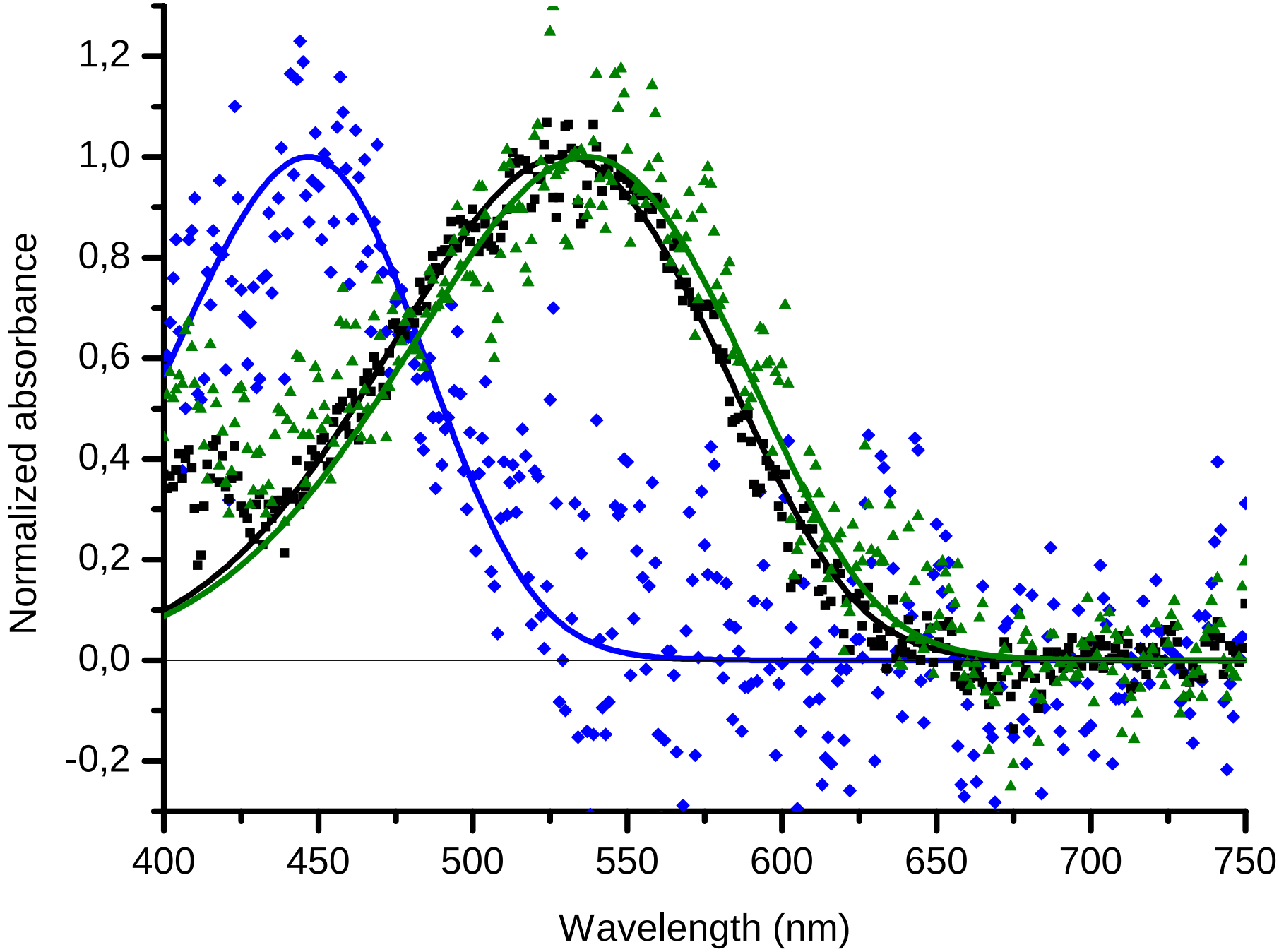

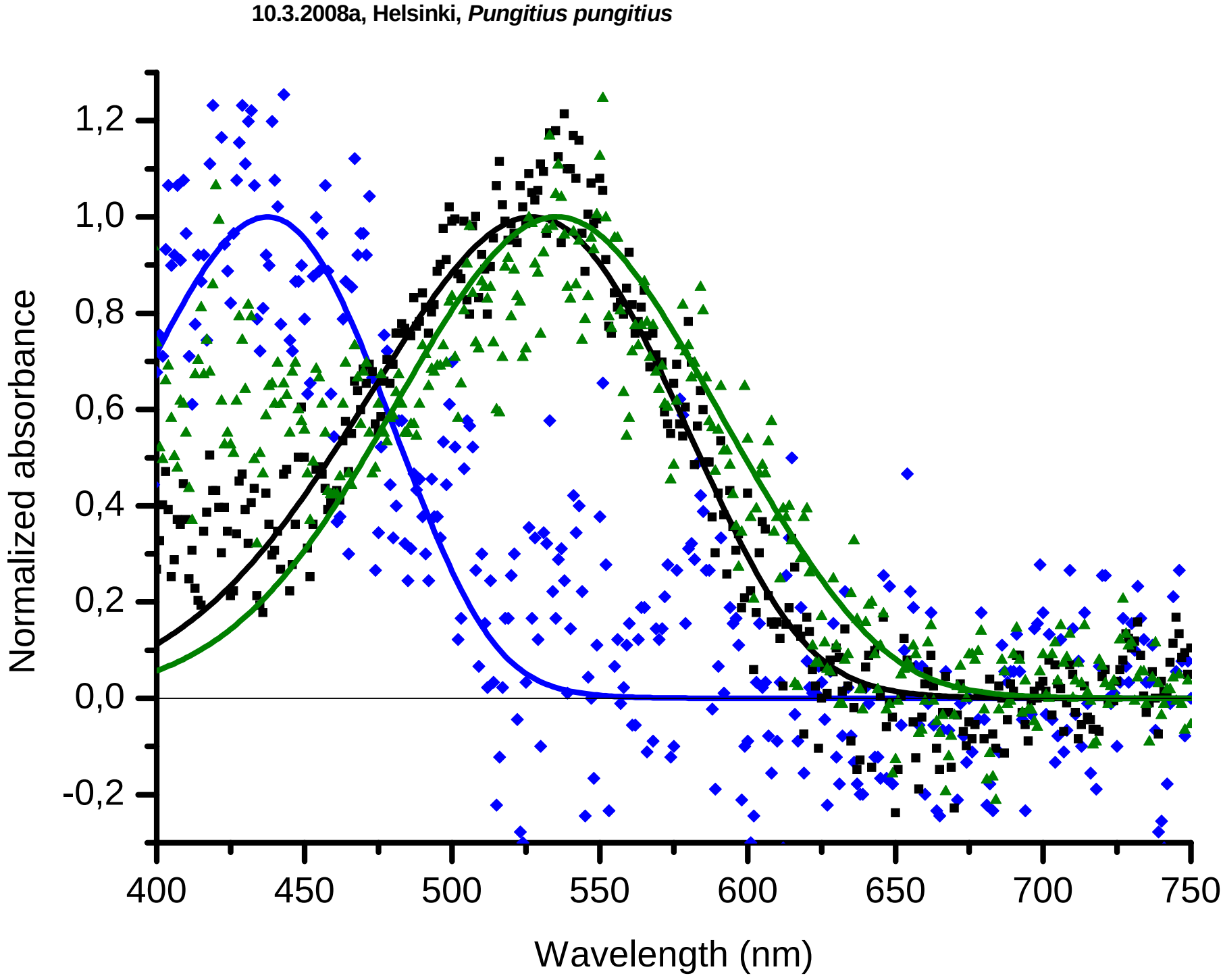
10.3.2008a, Helsinki, *Pungitius pungitius*
Normalized absorbance
1,2
1,0
0,8
0,6
0,4
0,2
0,0
-0,2
400
450
500
550
600
650
700
750
Wavelength (nm)

2.2.2011, Helsinki, *Pungitius pungitius*

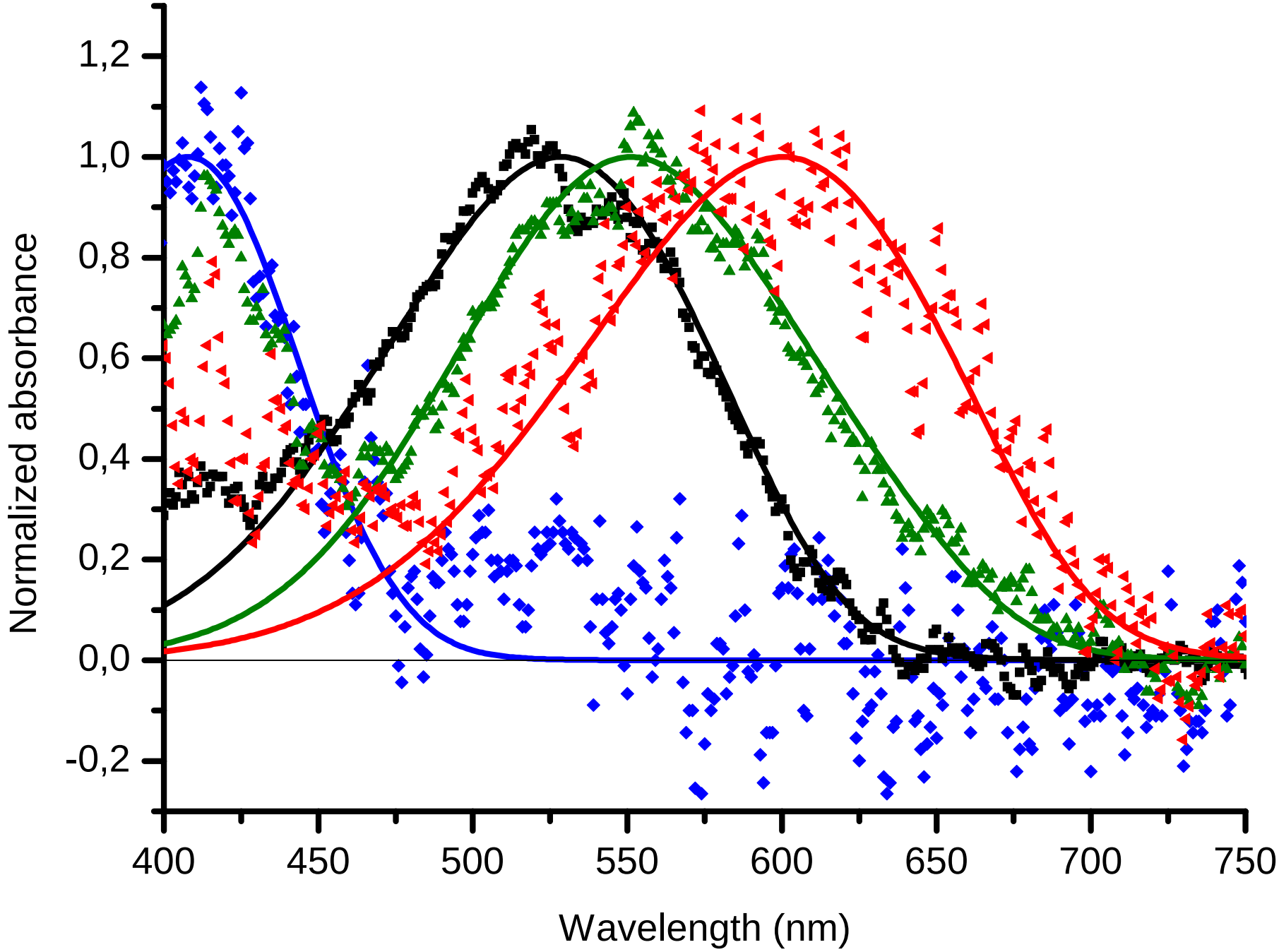

27.2.2008b, Iso-porontima, *Pungitius pungitius*

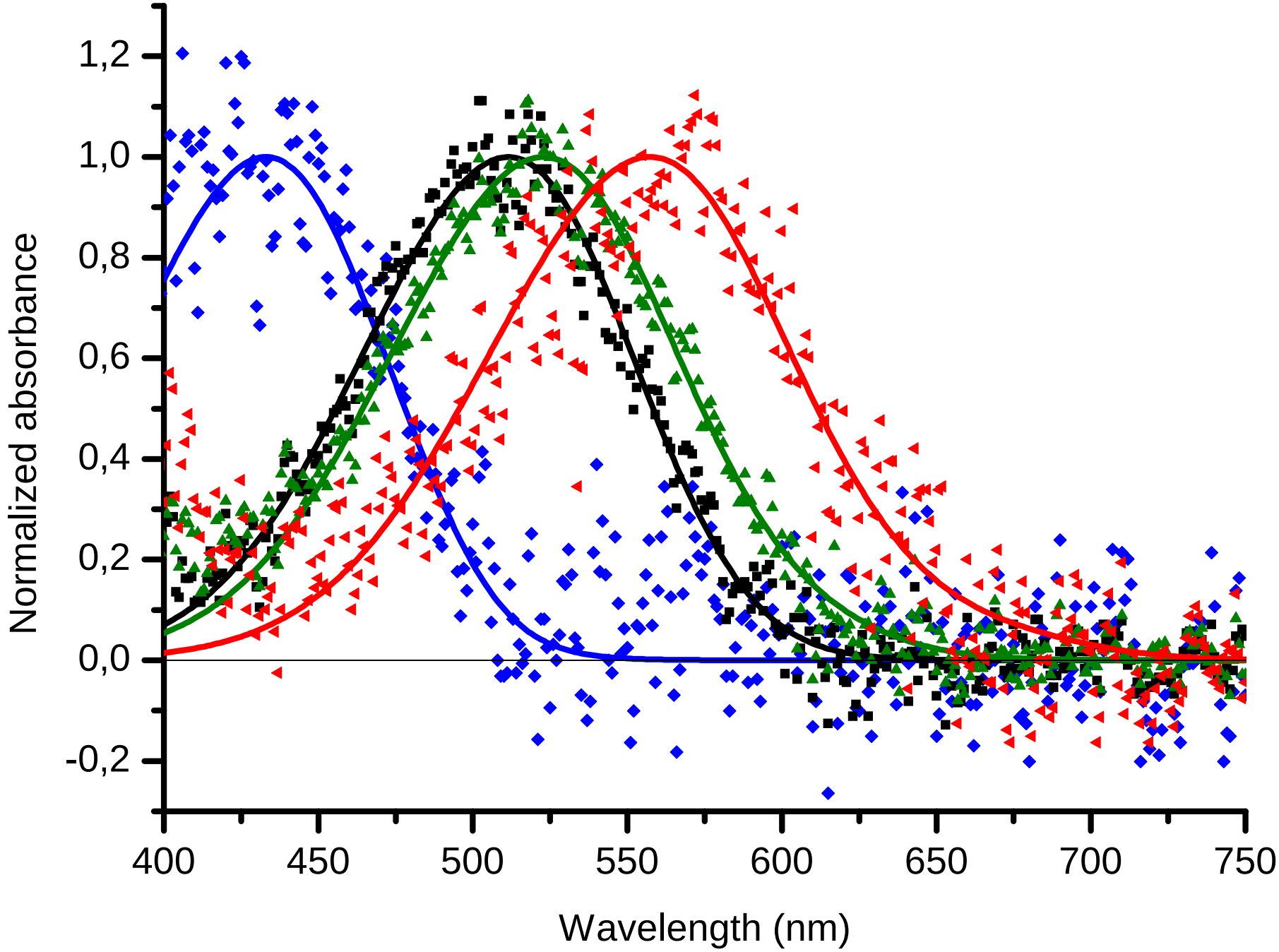

26.8.2008a, Mashinnoje, *Pungitius pungitius*

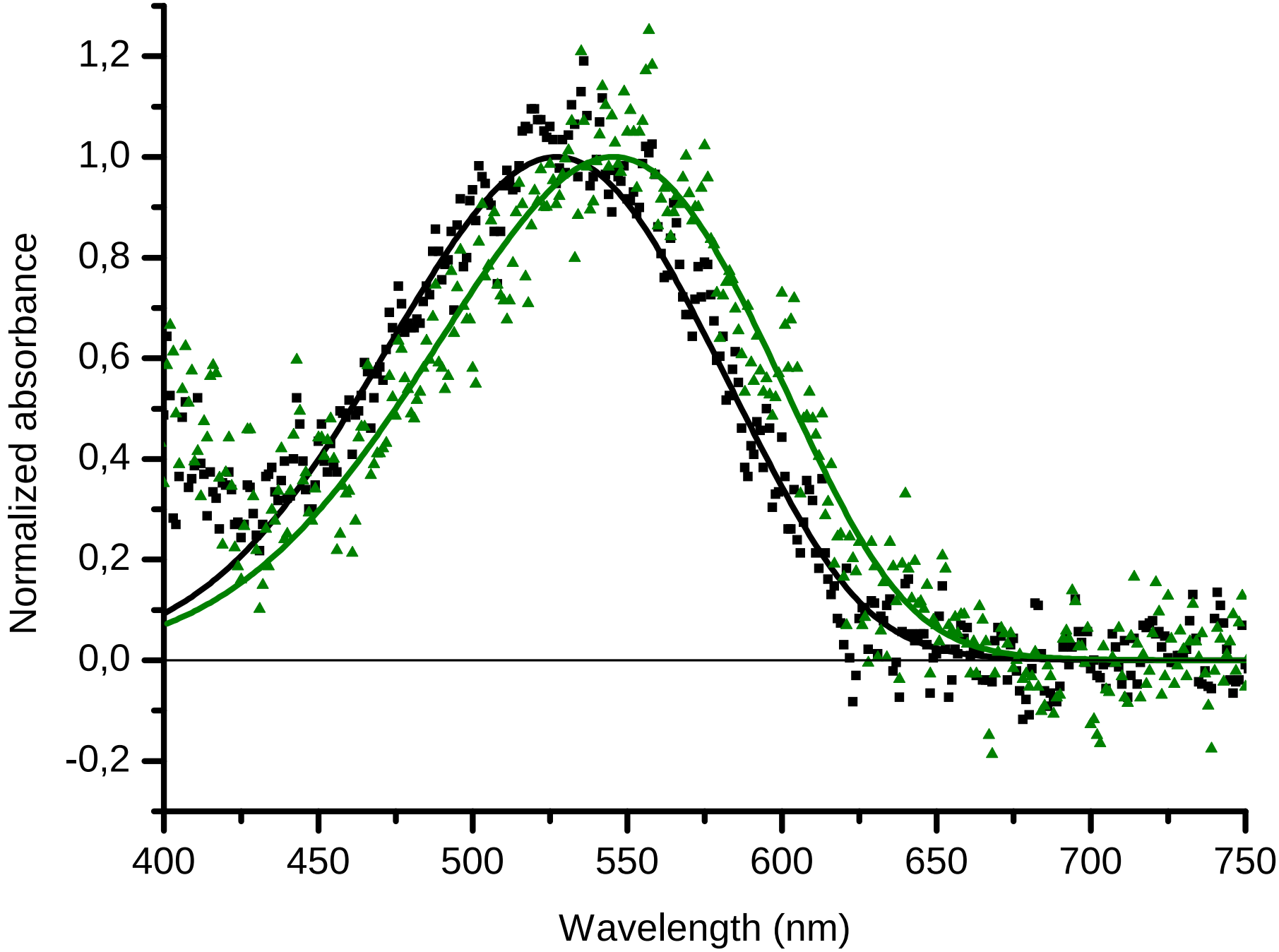

1.4.2008b, Pyöreälampi, *Pungitius pungitius*

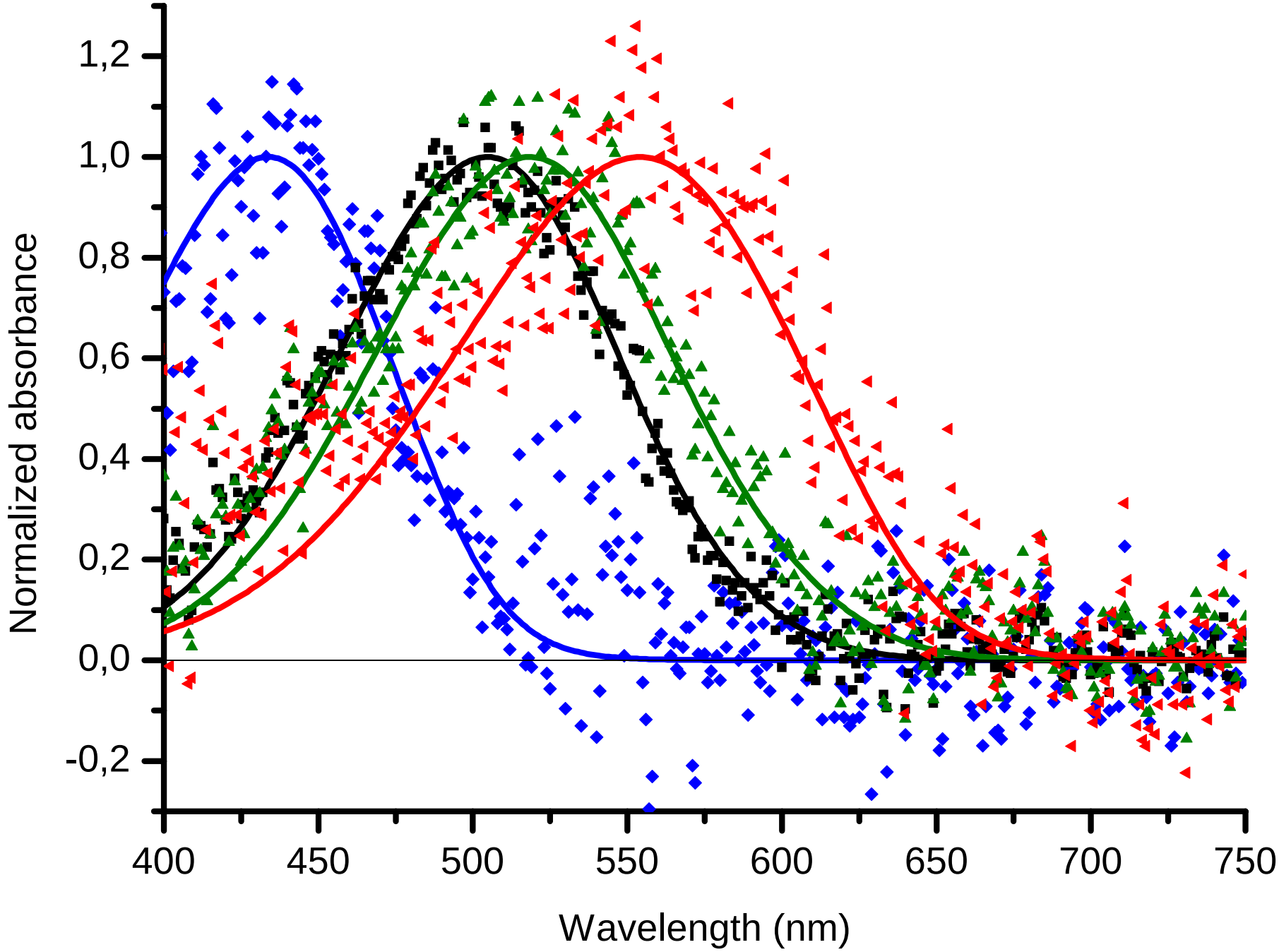

16.3.2011, Pyöreälampi, *Pungitius pungitius*

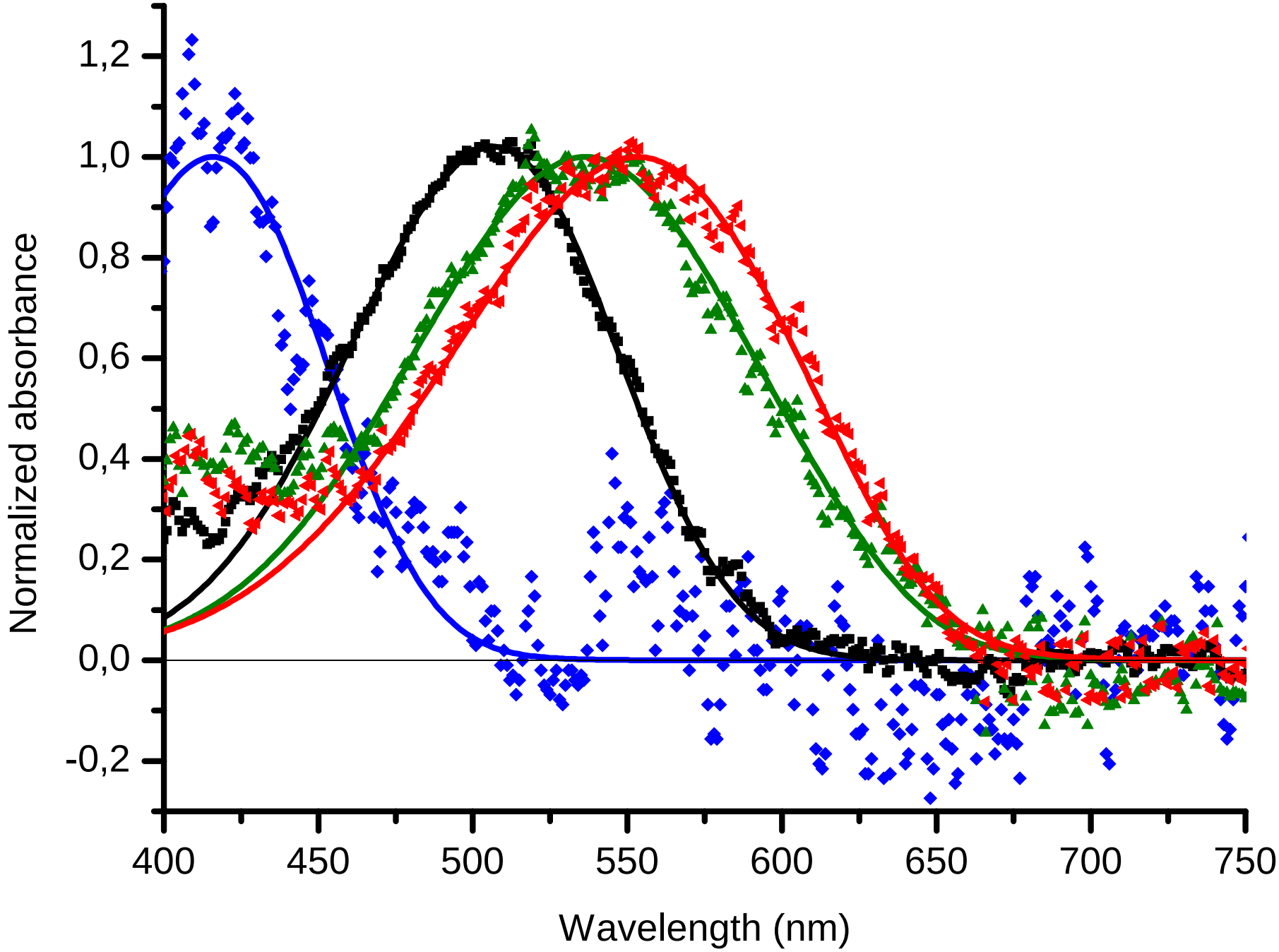

6.2.2008b, Rytilampi, *Pungitius pungitius*

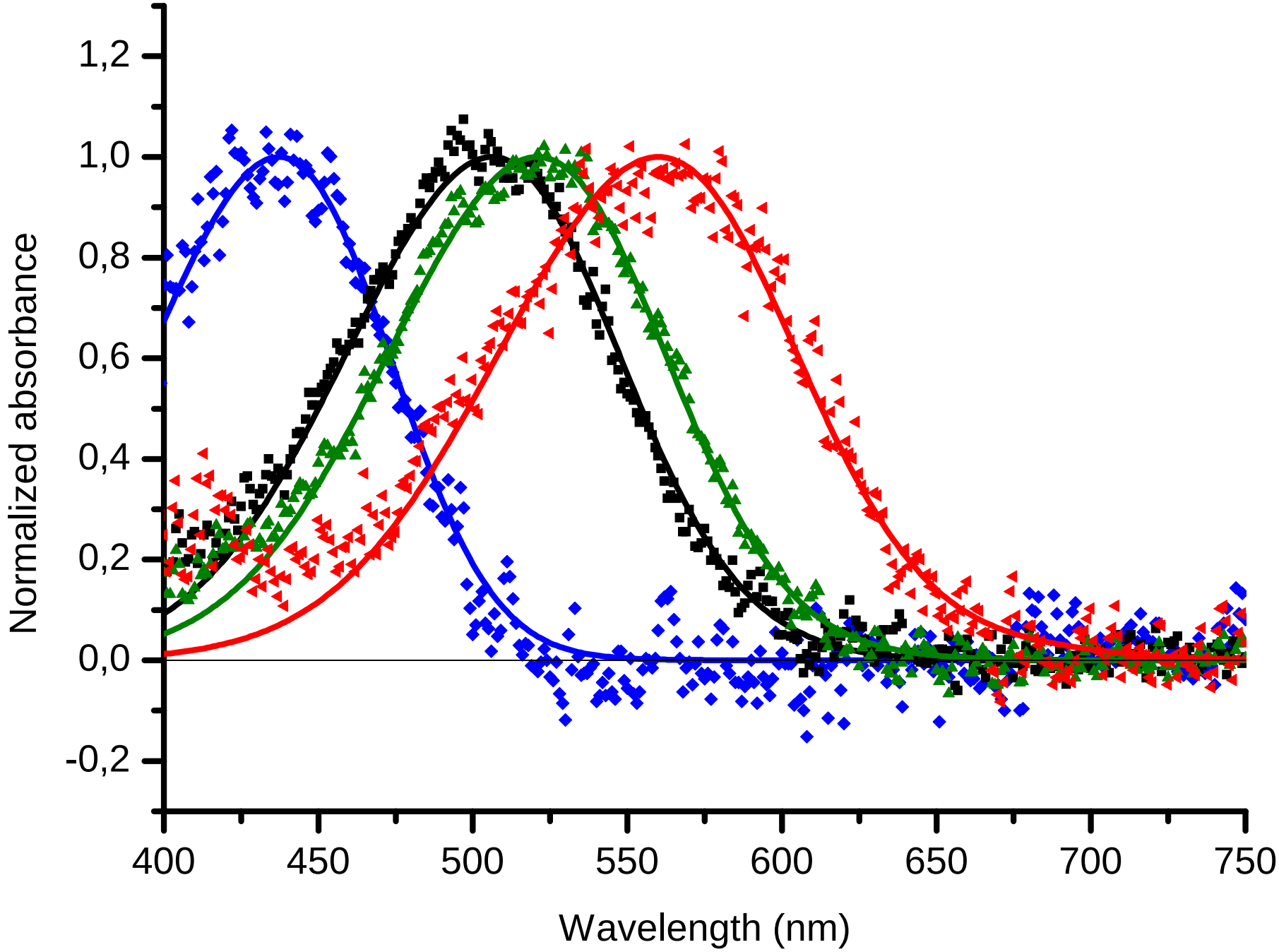

24.4.2008, White Sea, *Pungitius pungitius*